

Independent Optical Excitation of Distinct Neural Populations

Nathan C Klapoetke¹⁻⁵, Yasunobu Murata⁴⁻⁵, Sung Soo Kim⁶, Stefan R. Pulver⁶, Amanda Birdsey-Benson⁴⁻⁵, Yong Ku Cho¹⁻⁵, Tania K Morimoto¹⁻⁵, Amy S Chuong¹⁻⁵, Eric J Carpenter⁷, Zhijian Tian⁸, Jun Wang⁸, Yinlong Xie⁸, Zhixiang Yan⁸, Yong Zhang⁸, Brian Y Chow⁹, Barbara Surek¹⁰, Michael Melkonian¹⁰, Vivek Jayaraman⁶, Martha Constantine-Paton⁴⁻⁵, Gane Ka-Shu Wong^{7,8,11}, Edward S Boyden¹⁻⁵

¹ The MIT Media Laboratory, Synthetic Neurobiology Group, Massachusetts Institute of Technology, Cambridge, Massachusetts, USA

² Department of Biological Engineering, Massachusetts Institute of Technology, Cambridge, Massachusetts, USA

³ MIT Center for Neurobiological Engineering, Massachusetts Institute of Technology, Cambridge, Massachusetts, USA

⁴ Department of Brain and Cognitive Sciences, Massachusetts Institute of Technology, Cambridge, Massachusetts, USA

⁵ MIT McGovern Institute for Brain Research, Massachusetts Institute of Technology, Cambridge, Massachusetts, USA

⁶ Janelia Farm Research Campus, Howard Hughes Medical Institute, Ashburn, Virginia, USA

⁷ Department of Biological Sciences, University of Alberta, Edmonton, Alberta, Canada

⁸ Beijing Genomics Institute-Shenzhen, Shenzhen, China

⁹ Department of Bioengineering, University of Pennsylvania, Philadelphia, Pennsylvania, USA

¹⁰ Institute of Botany, Cologne Biocenter, University of Cologne, Cologne, Germany

¹¹ Department of Medicine, University of Alberta, Edmonton, Alberta, Canada

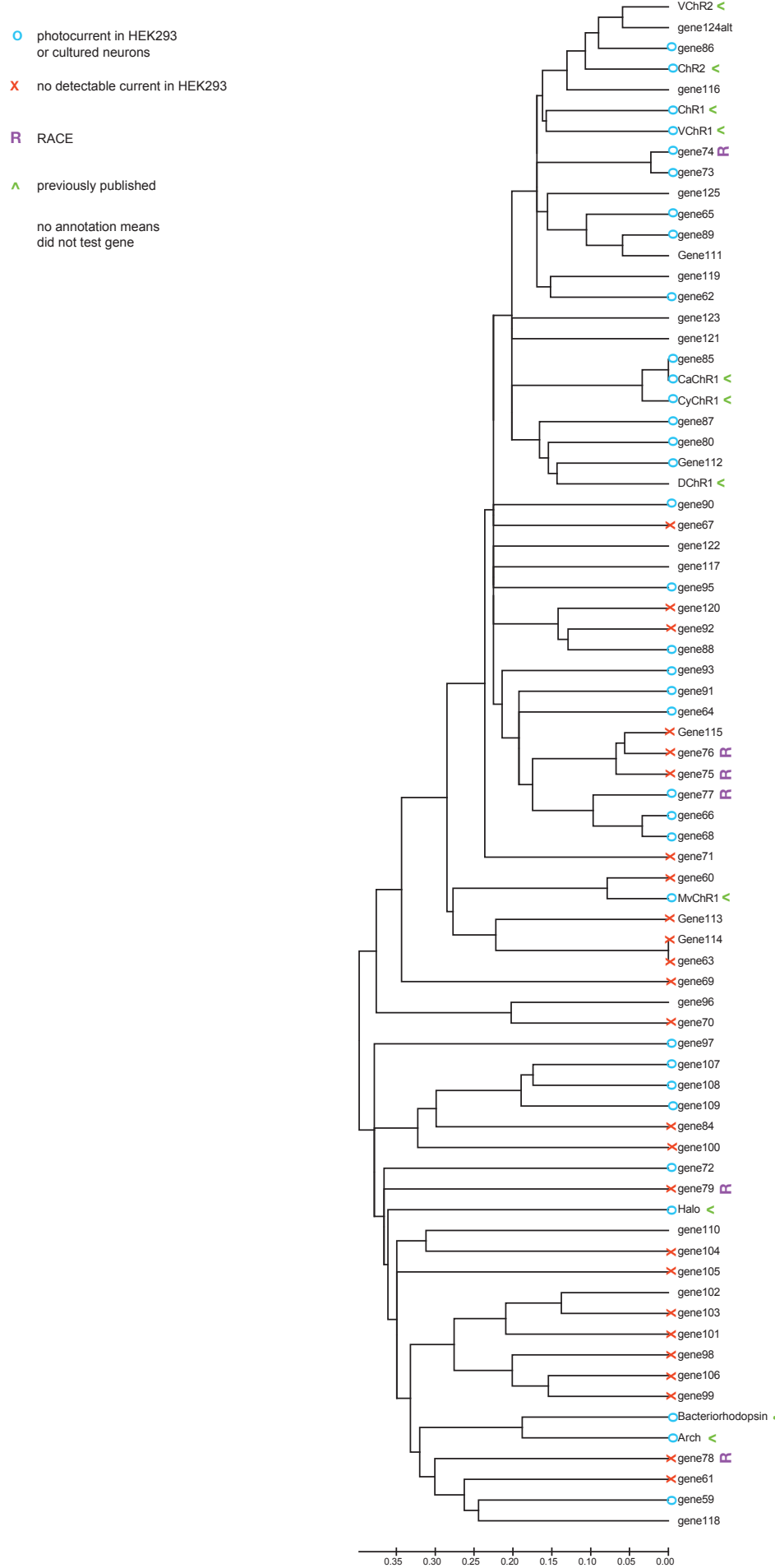
Co-corresponding authors, Edward S Boyden (esb@media.mit.edu), Gane KS Wong (gane@ualberta.ca)

Supplementary Figure 1	Phylogenetic relation of algal opsins.
Supplementary Figure 2	Sequence alignment.
Supplementary Figure 3	Characterization of channel kinetics of Chronos and Chrimson in HEK293FT cells.
Supplementary Figure 4	Comparison of ion selectivity of Chronos, Chrimson, and ChR2.
Supplementary Figure 5	Opsin screening in cultured neurons.
Supplementary Figure 6	Opsin trafficking in cultured neurons.
Supplementary Figure 7	Inactivation and recovery kinetics.
Supplementary Figure 8	Chronos full inactivation and recovery kinetics.
Supplementary Figure 9	ReaChR and Chrimson comparison in cultured neurons.
Supplementary Figure 10	Green light driven spiking frequency responses in cultured neurons.
Supplementary Figure 11	Electrical versus green light driven spiking fidelity in cultured neurons.
Supplementary Figure 12	Red light driven spiking in cultured neurons.
Supplementary Figure 13	Red and far-red spiking with ChrimsonR in acute cortical slice.
Supplementary Figure 14	Larval motor axons expressing ChR2 fire in response to blue but not red light pulses.
Supplementary Figure 15	Proboscis extension reflex (PER).
Supplementary Figure 16	Optogenetics of freely behaving intact flies.
Supplementary Figure 17	Two-color excitation controls in cultured neurons.
Supplementary Figure 18	Optically evoked post-synaptic currents (PSCs) in acute slice.
Supplementary Figure 19	Retina to superior colliculus projection stimulation with Chronos.
Supplementary Figure 20	Comparisons of spiking and post-synaptic response timing in acute slice.
Supplementary Figure 21	Optically evoked paired-pulse responses in acute slice.
Supplementary Figure 22	Post-synaptic current raw traces.
Supplementary Table 1	Naming convention
Supplementary Table 2	Primer sequences
Supplementary Video 1	Experimental setup with a visual arena.
Supplementary Video 2	PER of a Gr64f X Chrimson fly to 720 nm light in darkness.
Supplementary Video 3	Startle response to 720 nm light in darkness
Supplementary Video 4	PER of a Gr64f X Chrimson fly to 720 nm light in a blue random dot arena.
Supplementary Video 5	Inhibited startle response to 720 nm light in a blue random dot arena.
Supplementary Video 6	Optogenetics in freely behaving intact flies.

Supplementary Figure 1 – Phylogenetic relation of algal opsins.

Phylogenetic tree of novel opsins discovered from *de novo* transcriptomic sequencing of over 100 algal species. Only full length opsin sequences (i.e. has seven transmembrane helices) were analyzed. In some cases the transcriptome sequencing resulted in truncated opsin sequences, and rapid amplification of cDNA ends (RACE) was additionally performed on the original algal species to obtain the full length opsin sequence. See **Supplementary Table 1** for algal genus/species names, as well as the nicknames or aliases used in the main text of the paper (not all of the channelrhodopsins we obtained, were assigned nicknames or aliases, but instead are referred to just by number). Scale bar is the number of amino acid substitutions per site.

Supplementary Figure 1



Supplementary Figure 2 – Sequence alignment.

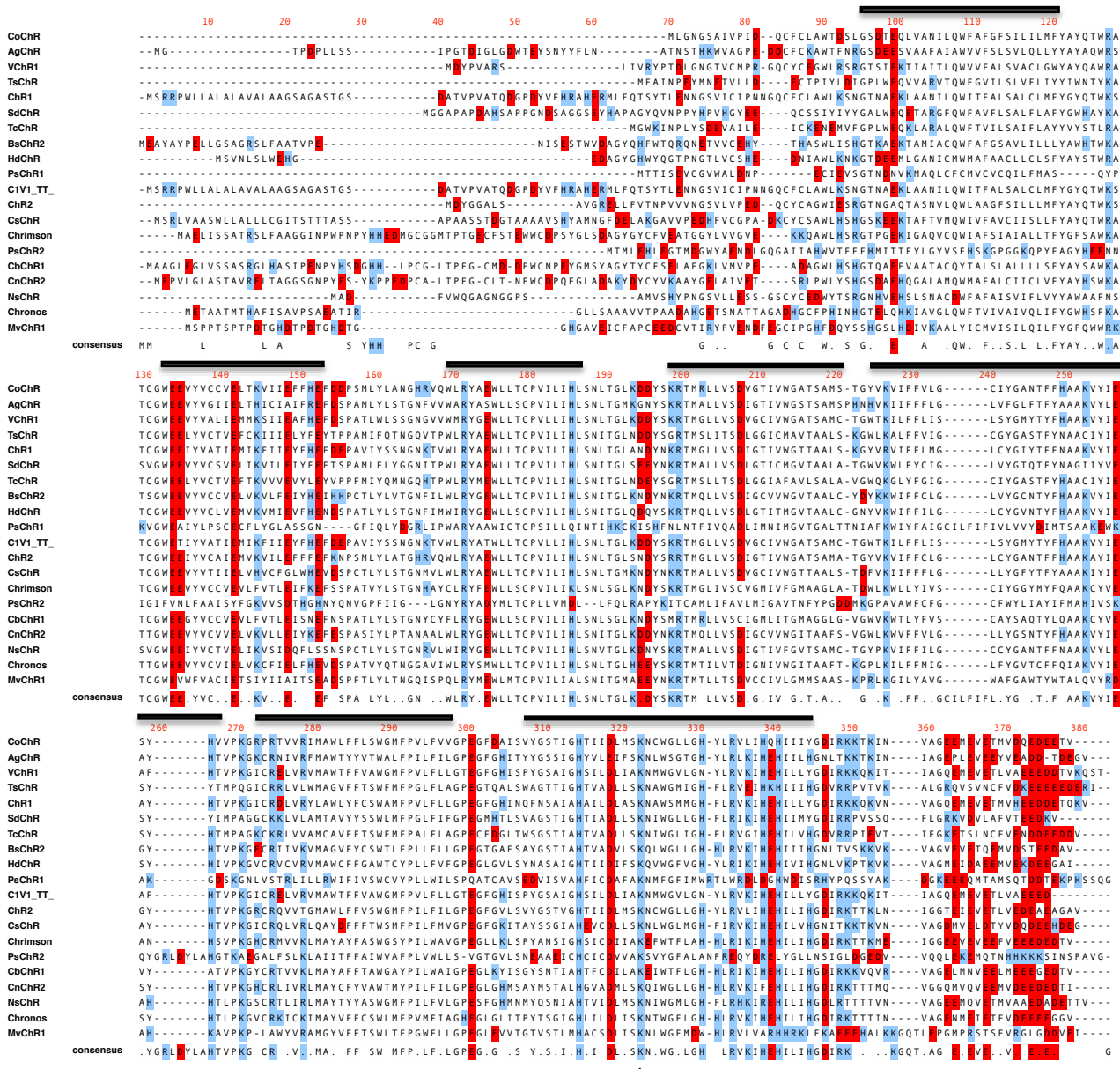
Protein sequence alignment of algal opsins screened in cultured neurons (Fig. 1).

Acidic residues are shown in red, basic residues are shown in blue.

Transmembrane regions are denoted by black bar above alignment based on

C1C2 crystal structure annotation. Schiff base lysine is annotated as *.

Supplementary Figure 2

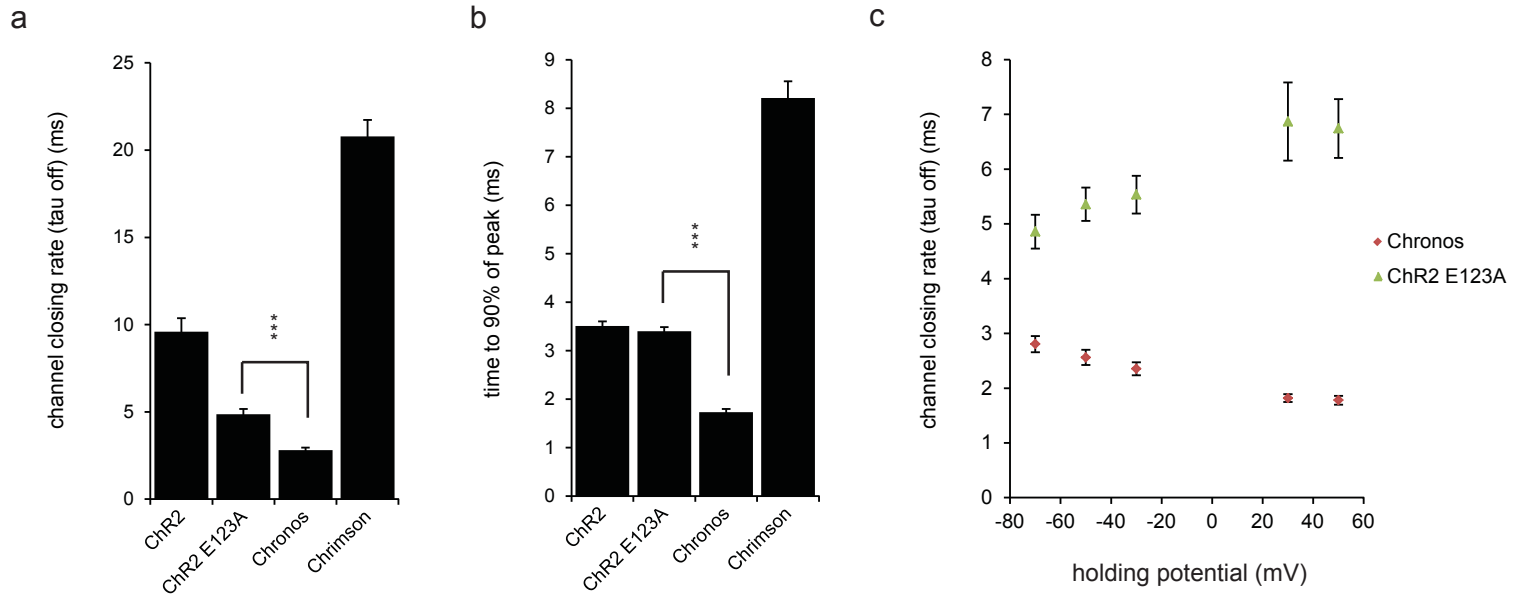


Supplementary Figure 3 – Characterization of channel kinetics of Chronos and Chrimson in HEK293FT cells.

(a-b) Population data for channel closing rate (τ_{off}) **(a)** and time to peak (time to reach 90% of peak photocurrent after the beginning of illumination) **(b)**, measured with 470 nm illumination and irradiance of 10 mW/mm², for ChR2, ChR2 E123A (aka ChETA_A), and Chronos, and 590 nm illumination and irradiance 4.6 mW/mm² for Chrimson ($n = 5 - 8$ HEK293FT cells each).

(c) Comparison of channel closing rate (τ_{off}) at various holding potentials for ChR2 E123A and Chronos, measured with 470 nm illumination, irradiance of 10 mW/mm². Pulse durations were 2 ms for panels **a**, **c**, and 1 s for panel **b**. Statistics for panels **a** and **b**: ***, $P < 0.001$, t-test comparing ChR2 E123A (ChETA_A) vs. Chronos. All data are plotted as mean \pm s.e.m. throughout.

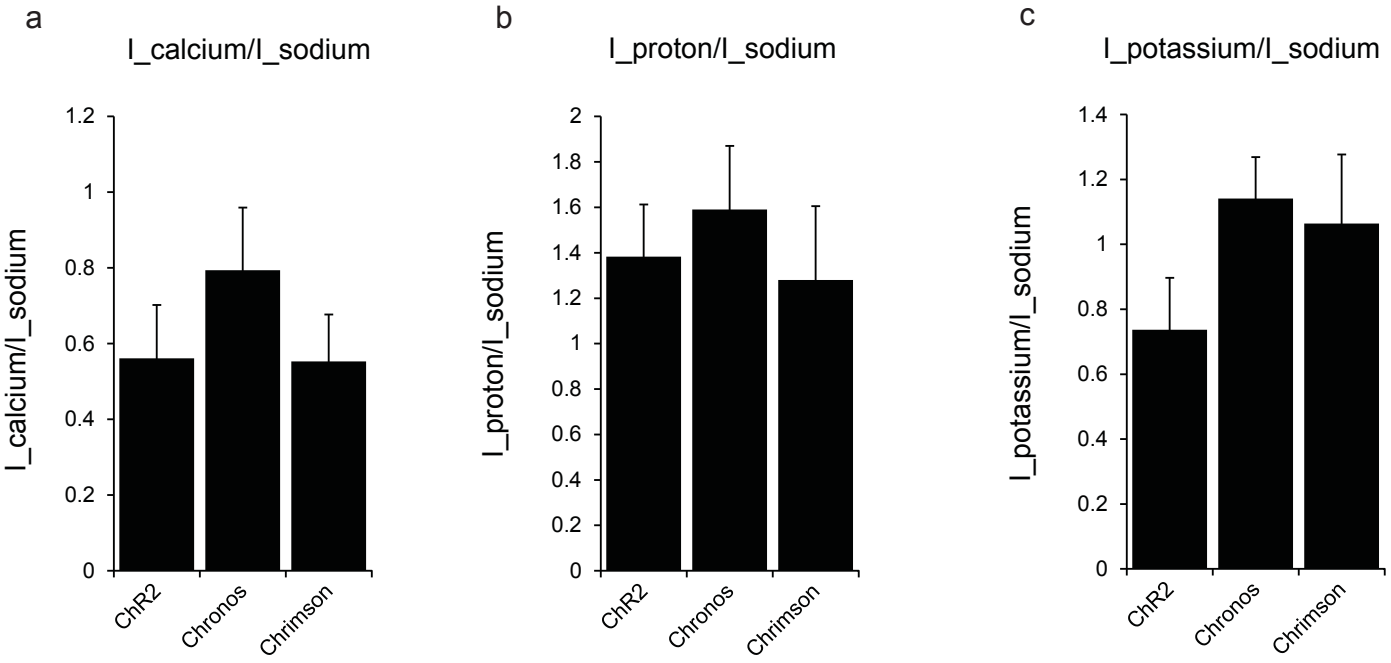
Supplementary Figure 3



Supplementary Figure 4 – Comparison of ion selectivity of Chronos, Chrimson, and ChR2.

(a-c) Population data for photocurrent density ratios, measured using whole-cell patch clamp in HEK cells in ion-specific extracellular solutions (see **Methods**); using 1 s illumination of 470 nm, irradiance of 10 mW/mm² for ChR2 and Chronos, 1s illumination of 590 nm, irradiance of 4.6 mW/mm² for Chrimson. Shown is data for ChR2, Chronos, and Chrimson ($n = 6 – 10$ HEK293FT cells each). **(a)** Calcium photocurrent (I_{calcium}) measured in 90 mM CaCl₂, pH 7.4, vs. sodium photocurrent (I_{sodium}) measured in 145 mM NaCl, pH 7.4. **(b)** Proton photocurrent (I_{proton}) measured in 135 mM NMDG, pH 6.4 vs. sodium photocurrent (I_{sodium}). **(c)** Potassium photocurrent ($I_{\text{potassium}}$) measured in 145 mM KCl, pH 7.4 vs. sodium photocurrent (I_{sodium}).

Supplementary Figure 4



Supplementary Figure 5 – Opsin screening in cultured neurons.

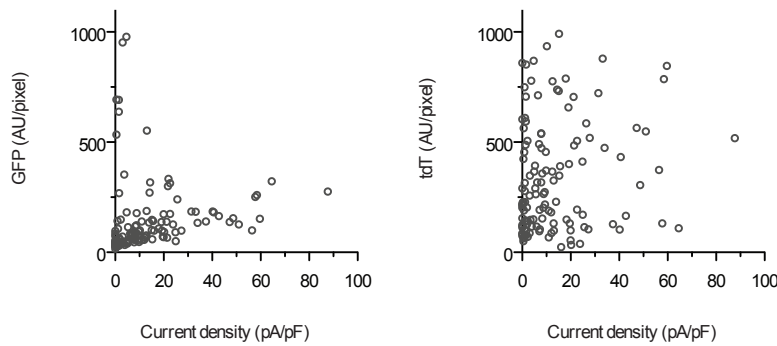
(a) Comparison of fluorescence and current density across all opsins screened.

Each dot represents the data from a cell expressing one of the opsins in Fig. 1, pooled over all opsins. Photocurrent was measured for each opsin with the wavelength nearest its peak using 5 ms pulses (equal photon fluxes across wavelength; 470 nm, 4.23 mW/mm²; 530 nm, 3.66 mW/mm²; 625 nm, 3.14 mW/mm²). **(b)** Opsin-GFP and tdTomato fluorescence for each construct patched and the membrane parameters indicated on the y-axes ($n = 3 – 12$ cells each).

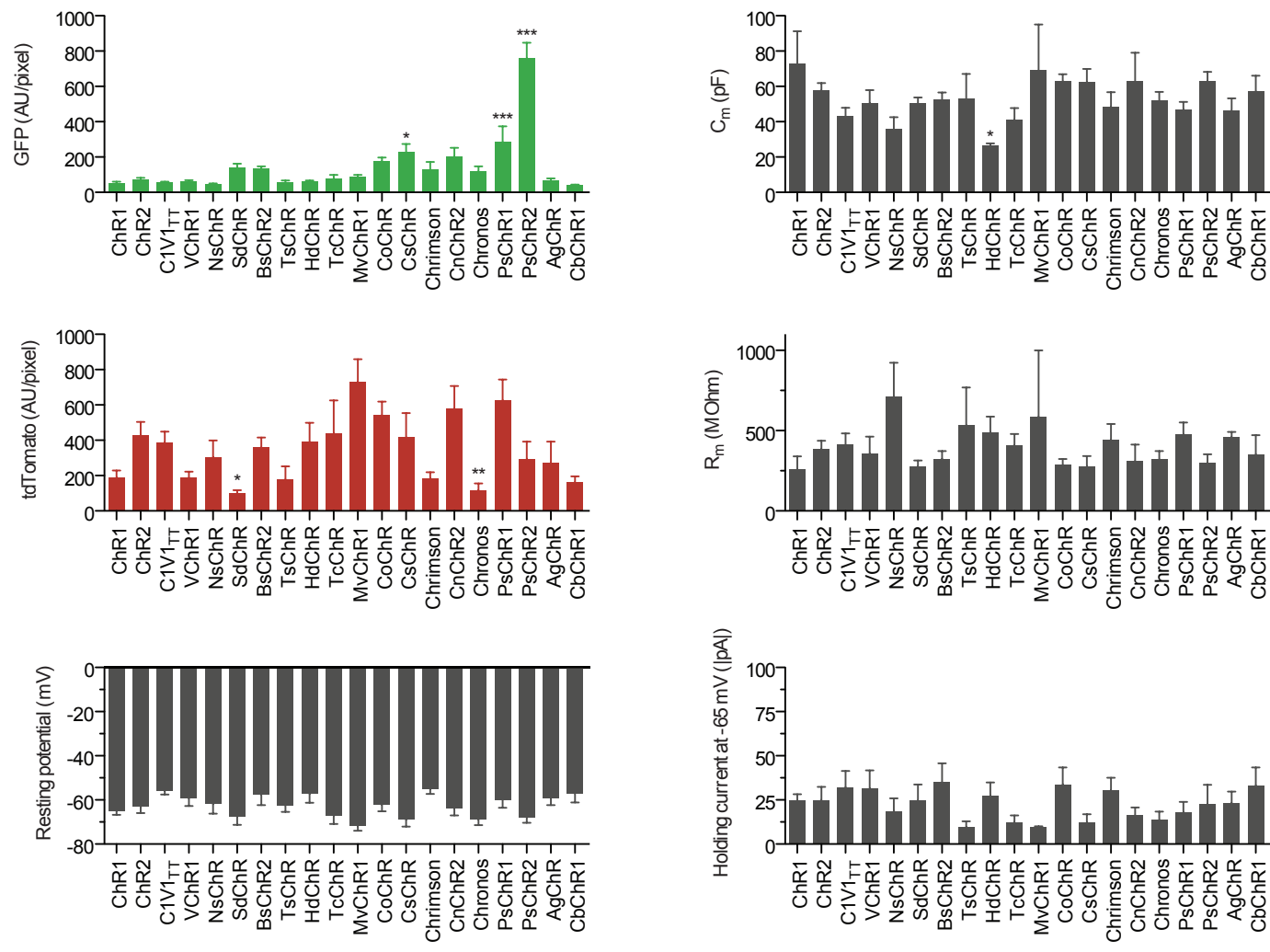
(c) Photocurrent measured at equal photon fluxes using 5 ms pulses (same irradiances as part **a**: $n = 6$ CsChR cells, $n = 2$ C1V1_{TT} cells, $n = 8$ Chrimson cells). **(d)** Action spectra in HEK293FT cells done under the same conditions as Fig. 1g. Statistics for panels **b**: $^*P < 0.05$, $^{**}P < 0.01$ and $^{***}P < 0.001$, ANOVA with Dunnett's post hoc test, with ChR2 as the reference.

Supplementary Figure 5

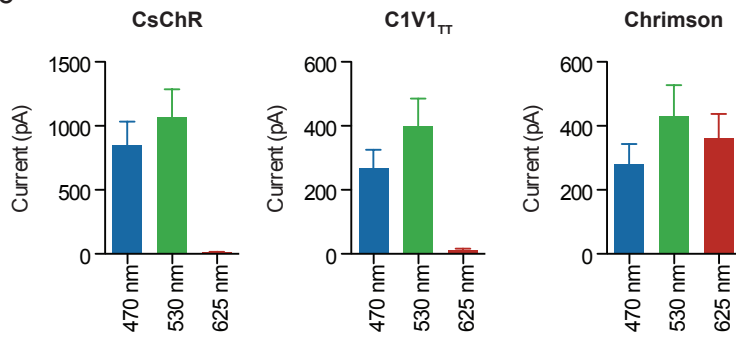
a



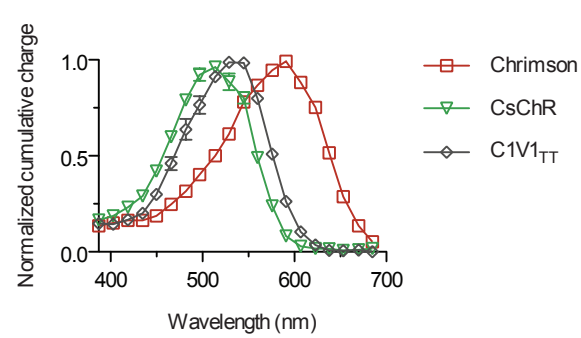
b



c



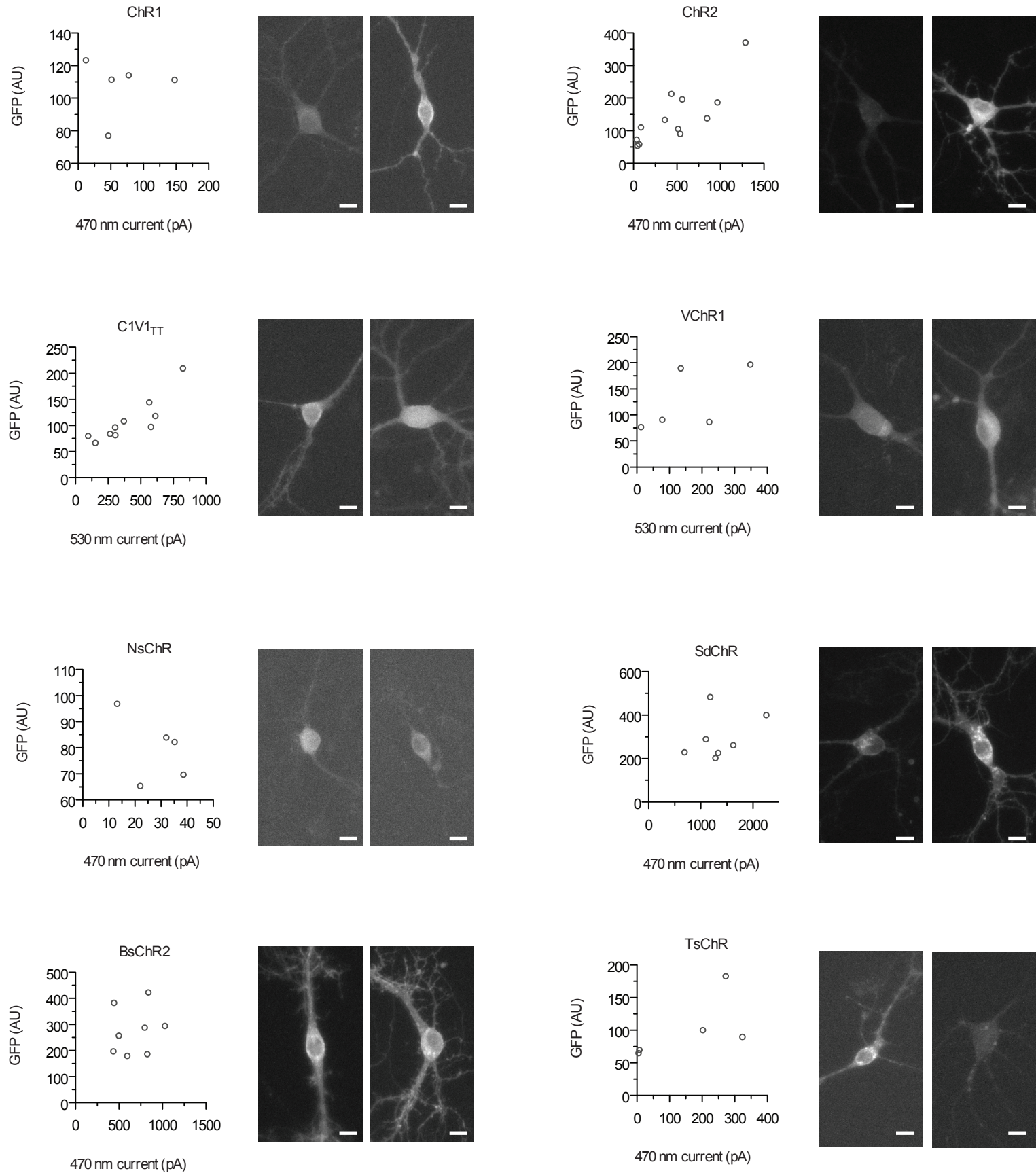
d

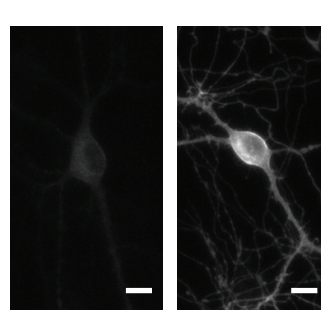
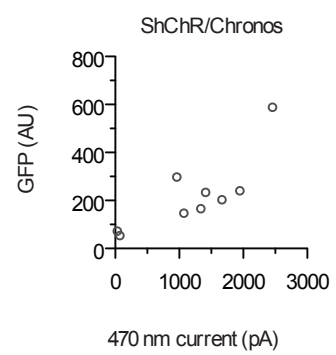
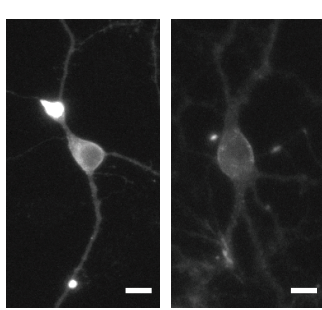
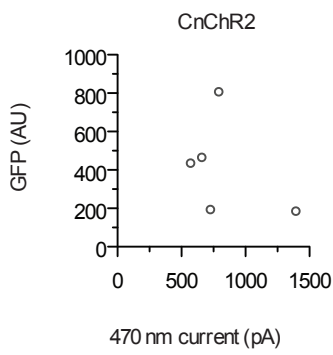
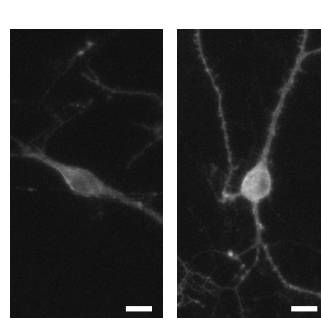
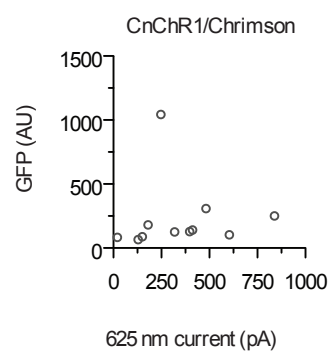
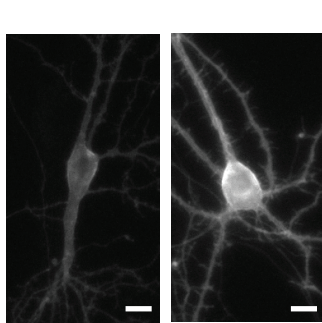
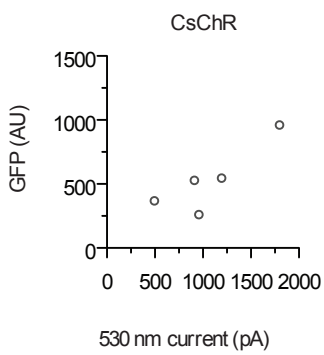
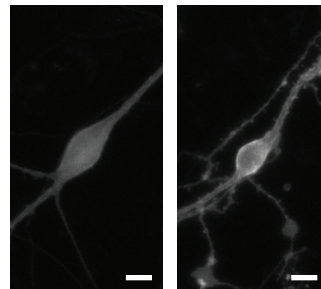
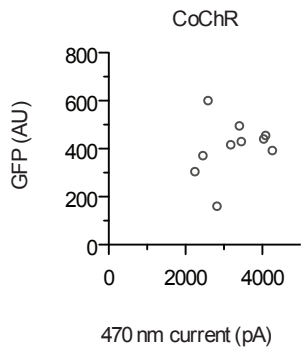
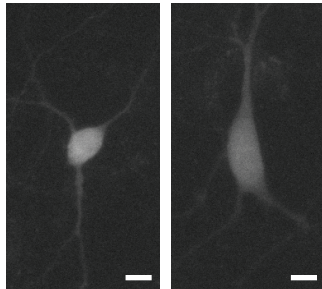
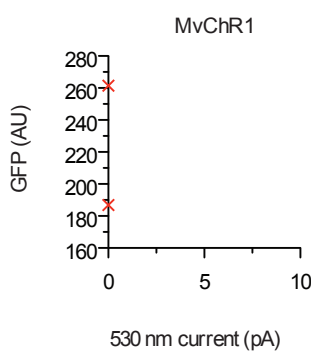
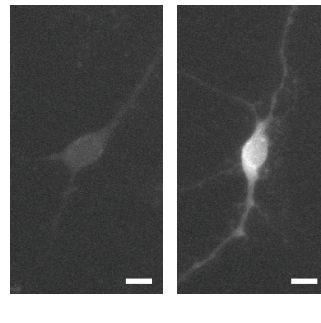
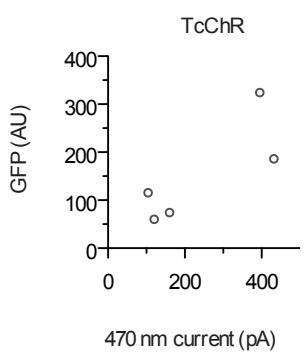
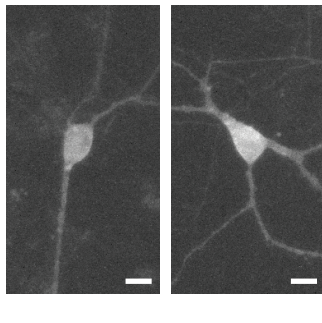
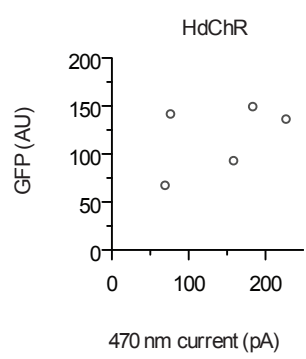


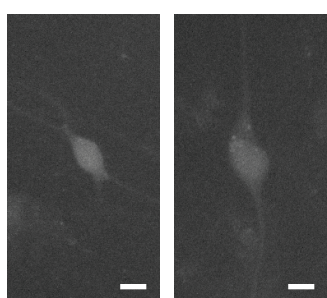
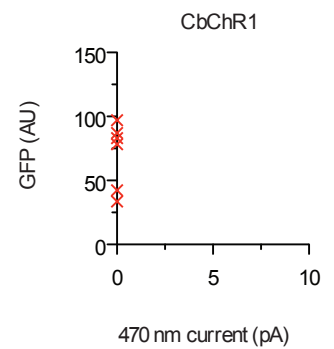
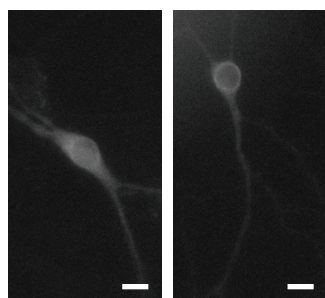
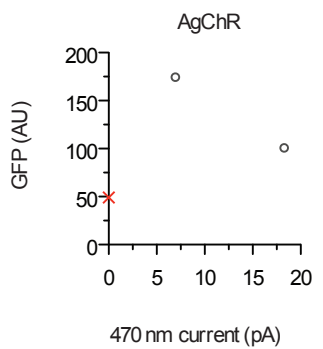
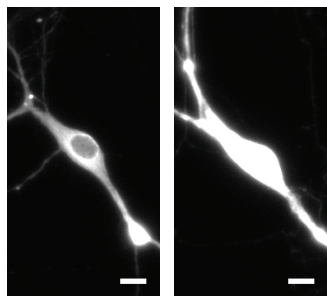
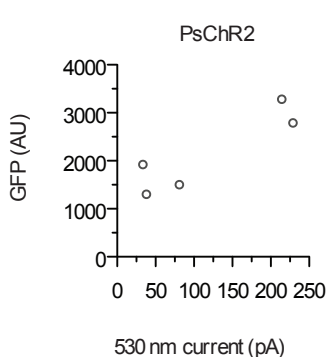
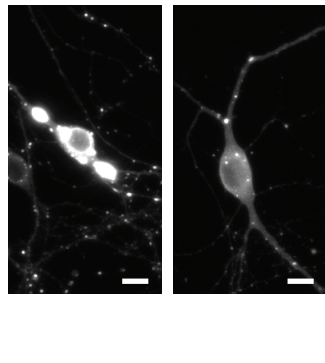
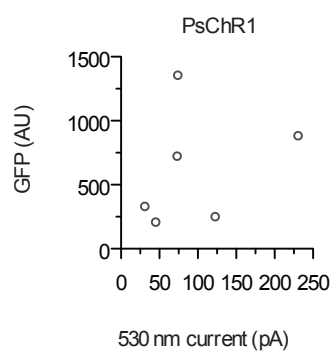
Supplementary Figure 6 – Opsin trafficking in cultured neurons.

Channelrhodopsin trafficking and photocurrent comparison from cultured neuron screening. Quantitative soma GFP fluorescence versus current measured at the light power of peak sensitivity (same conditions as Supplementary Fig. 5a) for each neuron experimented on (indicated by a circle) (left), GFP images for the median current (middle) and maximum current (right) cells are shown for each opsin. Scale bar, 10 µm. Note that in the GFP versus current plot, the GFP intensity values are absolute, and thus can be compared across opsins. However due to two-log-unit variance in absolute GFP intensity, the brightness and contrast settings used for the median images are varied across the different opsins, so the GFP images should not be used to compare brightness across constructs. That said, the brightness and contrast settings for each opsin's median and maximum current cells are matched, to illustrate whether higher expression correlates with increased photocurrent. See Methods for imaging conditions and **Supplementary Table 1** for full genus/species names.

Supplementary Figure 6



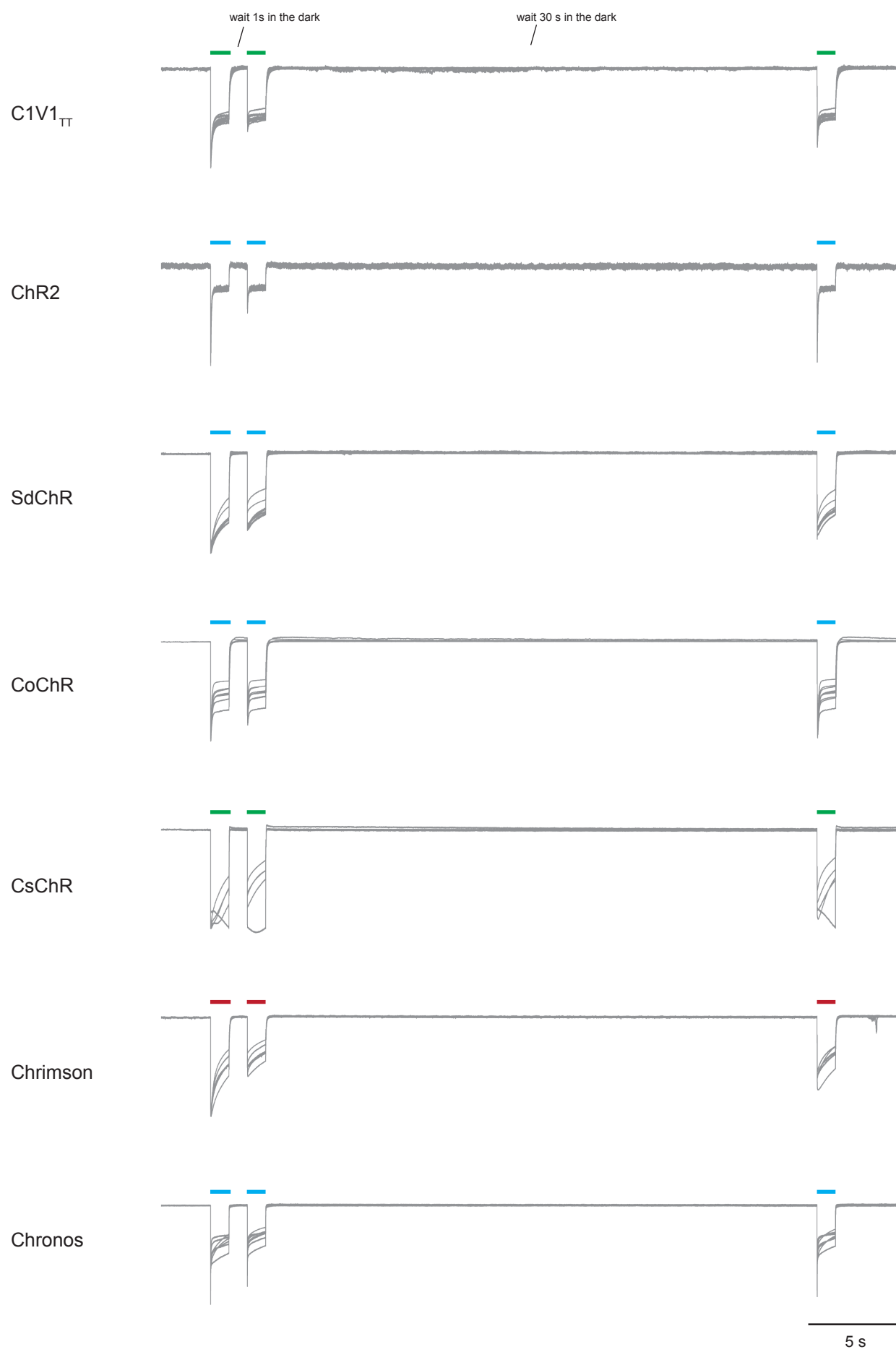




Supplementary Figure 7 – Inactivation and recovery kinetics.

Normalized traces of photocurrent recovery kinetics, with traces from each patched cell overlaid, with experiments as performed in **Fig. 1j**.

Supplementary Figure 7

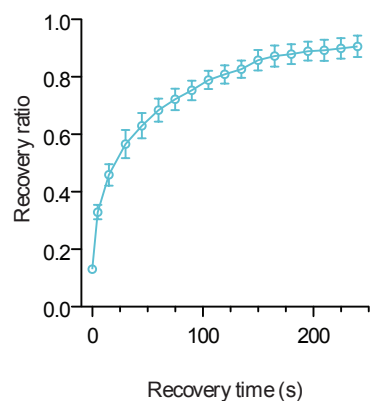


Supplementary Figure 8 – Chronos full inactivation and recovery kinetics.

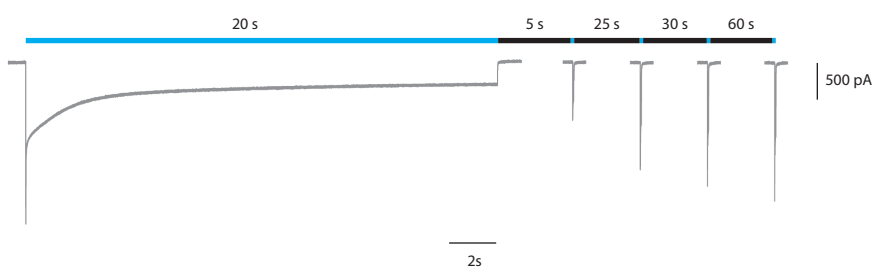
(a) Peak current recovery ratio vs. waiting time in darkness after 20 s of illumination ($n = 3$ cells), followed by a variable period of darkness, and assessed with a 50 ms pulse. **(b)** Representative trace showing Chronos inactivation has a fast and a slow component under continuous illumination.

Supplementary Figure 8

a



b



Supplementary Figure 9 – ReaChR and Chrimson comparison in cultured neurons.

Side-by-side comparisons of Chrimson and ReaChR's spectral sensitivity.

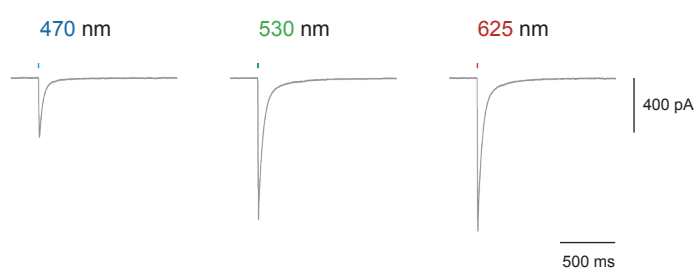
tdTomato was co-expressed with opsin-GFP for unbiased selection of neurons.

(a-d) Raw traces and photocurrent measurements at equal photon fluxes across wavelengths. Red (625 nm) measurement was done before other wavelengths to avoid potential inactivation ($n = 5$ cells; 5 ms pulse; 470 nm, 4.23 mW/mm²; 530 nm, 3.66 mW/mm²; 625 nm, 3.14 mW/mm²). **(e)** Short vs. long pulse activation of ReaChR at 625 nm. Raw traces from a representative cell showing current in response to a 5 ms (left) vs. 1 s (middle) pulse of red light. Additional dashed lines on the 1 s pulse trace correspond to the current amplitude at the indicated time post-light-onset. Individual cell data is plotted on the right ($n = 4$ cells; 5 ms, 3.14 mW/mm²; 1 s, 5 mW/mm²). **(f)** Turn-on kinetics comparison in response to a 1 s pulse. ($n = 4 - 6$ cells; 625 nm, 5 mW/mm²).

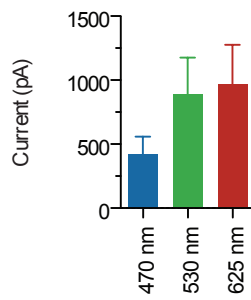
Supplementary Figure 9

a

Chrimson 5 ms pulse

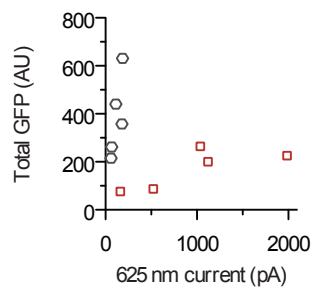


Chrimson



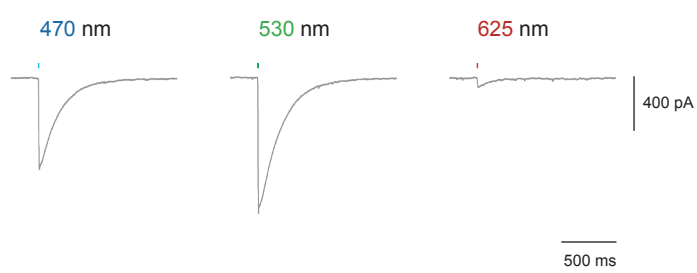
b

□ Chrimson ○ ReaChR

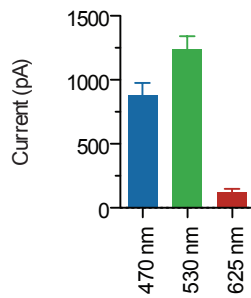


c

ReaChR 5 ms pulse

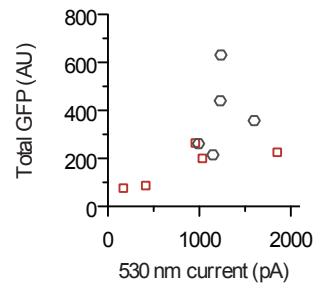


ReaChR



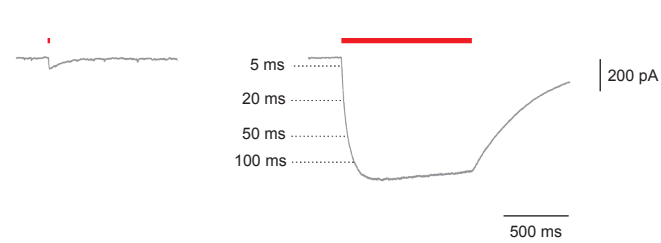
d

□ Chrimson ○ ReaChR

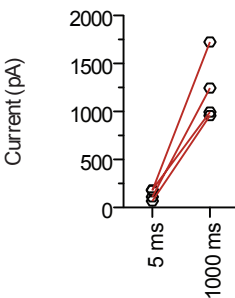


e

ReaChR 5 ms vs. 1000 ms pulse

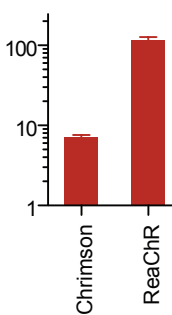


ReaChR 625 nm



f

625 nm 1000 ms



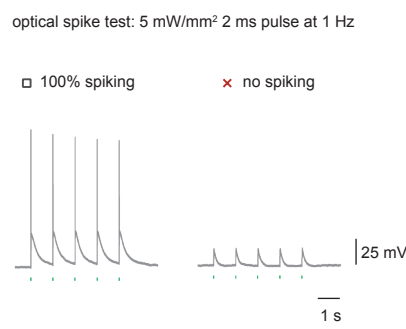
**Supplementary Figure 10 – Green light driven spiking frequency responses
in cultured neurons.**

(a-b) tdTomato was co-expressed with opsin-GFP for unbiased selection of neurons to patch. Any neuron that could not drive a train of 1 Hz, 10 pulses, of green (530nm) light at 5 mW/mm² with 100% spike probability was excluded from further spike frequency analysis, since the focus here was on high spike frequency fidelity. Generally neurons that could not drive spikes at 1Hz (indicated by red X's, as depicted in **a**) had lower GFP intensity than the neurons that could (indicated by black squares), in **b**. Each symbol is one cell. **(c)** Comparison of current measured at the end of 1 s green light (5 mW/mm²), defined as I_{min} in the trace (left). Asterisk indicates escaped spike-like sodium current since TTX was not used. J_{min} is I_{min} divided by membrane capacitance. Symbols are defined in the same manner as in **a-b**. **(d-h)** Characterization of green light driven spike frequency responses for cells that passed the 1 Hz spiking test in **a-b**. Stimulation train consisted of 40 pulses of green light in all cases ($n = 5 – 8$ cells for each opsin). **(d)** Individual cell spike probability vs. frequencies over irradiances. Population summary is shown on the right. **(e)** Population data for spike fidelity within the 40 pulse stimulation train. **(f)** Individual cells' spike latency, defined as time from light onset to spike peak. **(g)** Membrane parameter controls to show that the observed spiking differences were not due to changes in neural excitability. **(h)** Comparison of measured and projected current density to estimate the effective driving force during optical spiking for cells that passed

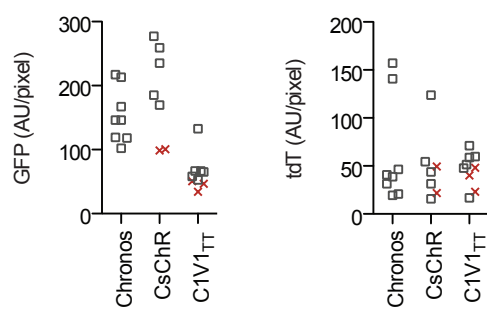
the 1 Hz spiking test in **a-c**. Measured current density J_{\min} is the same data set as panel **c**. Projected current densities (J_{\max} , J_{\max} for 2 ms pulse) are calculated by multiplying the measured J_{\min} (from **h**) by the ratios (J_{\max}/J_{\min} or J_{\max} for 2 ms/ J_{\min}) derived under the same illumination conditions but with TTX blockade (see **Supplementary Fig. 7**, for TTX data). “ J_{\max} for 2 ms pulse” refers to the maximum current density within the 2 ms post-light-onset interval. Statistics for panels **h**: $^*P < 0.05$, $^{**}P < 0.01$ and $^{***}P < 0.001$, ANOVA with Dunnett’s post hoc test, with C1V1_{TT} as the reference.

Supplementary Figure 10

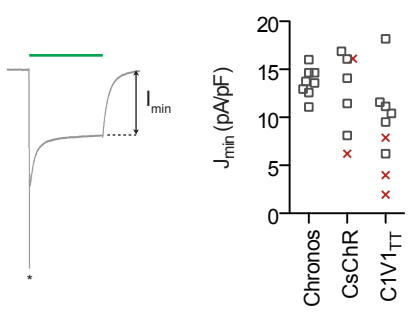
a



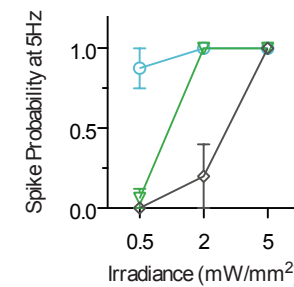
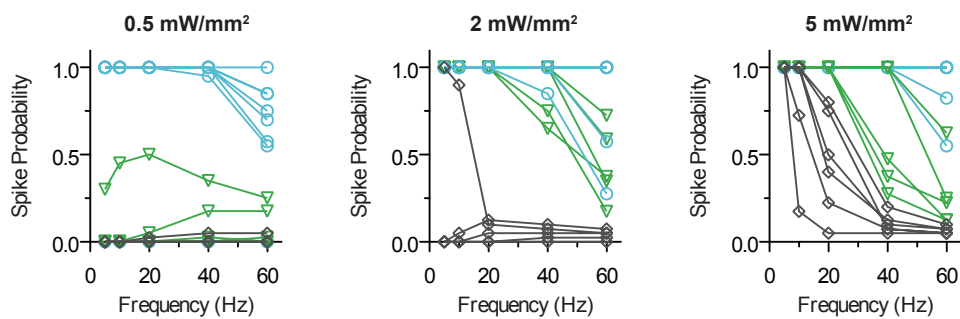
b



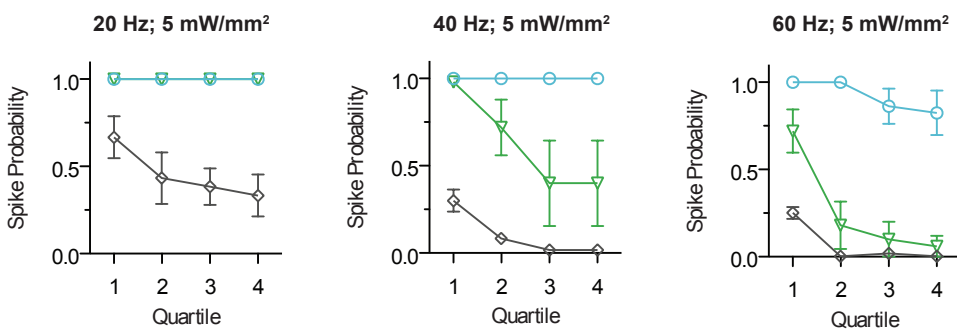
c



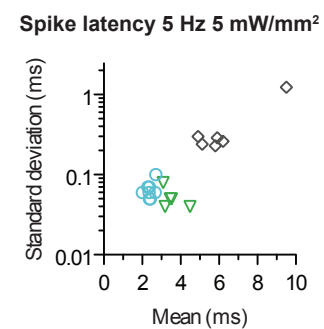
d



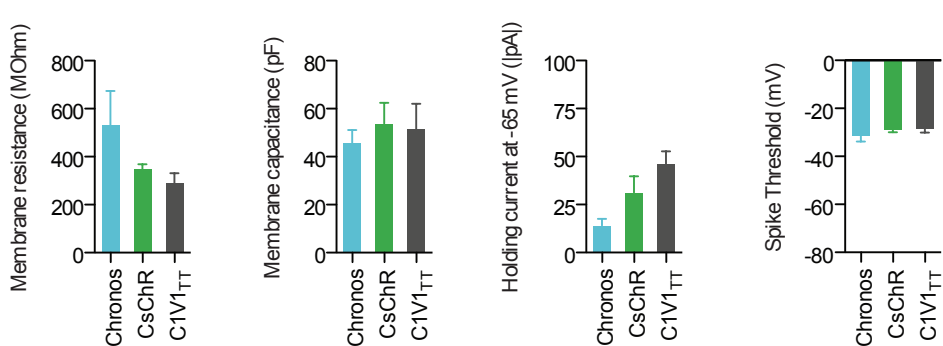
e



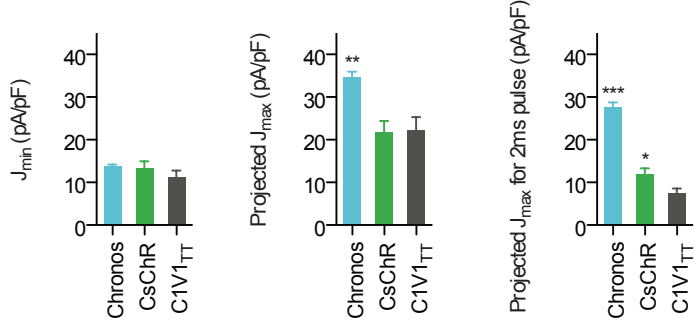
f



g



h

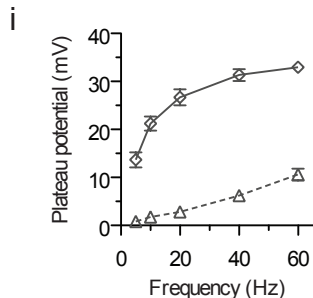
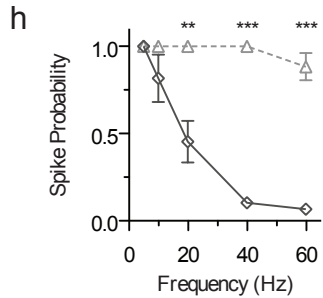
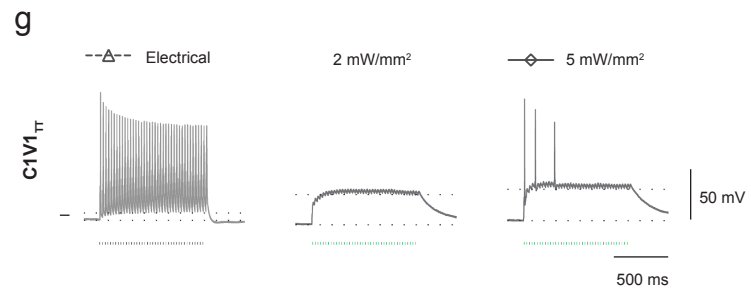
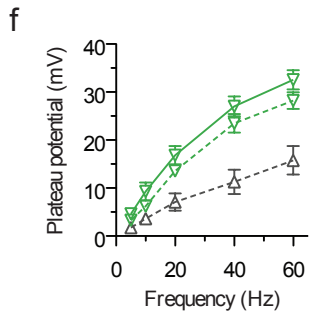
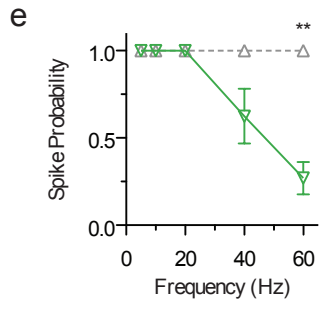
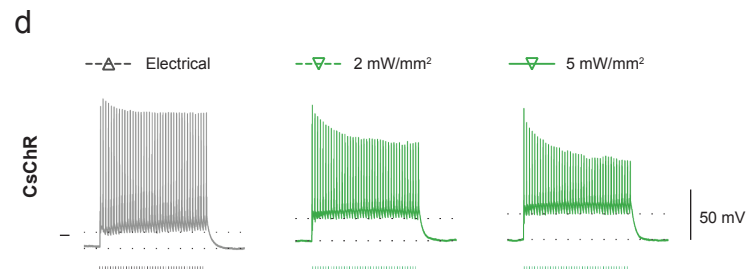
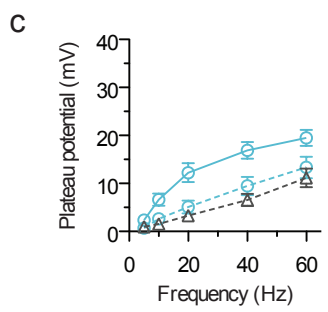
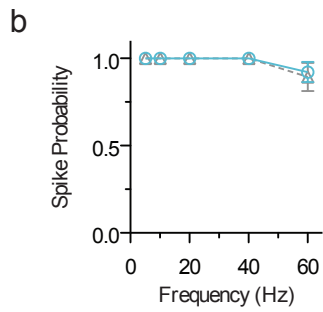
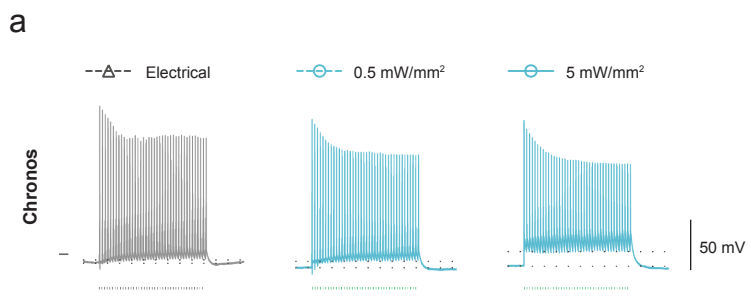


Supplementary Figure 11 – Electrical versus green light driven spiking fidelity in cultured neurons.

Additional analysis of optical versus electrical spike probability over various frequencies at 5 mW/mm²; same dataset as **Supplementary Fig. 10d-h**.

Electrical stimulation protocol was the same as optical, except the pulse duration was 5 ms and the input current was varied between 200-800 pA to maximize spike probability. Plateau potential was measured as the voltage difference between two horizontal dotted lines as shown in each trace. A single dash to the left of electrical traces indicates -65 mV. Statistics for **b**, **e**, and **h**: Paired t-test between electrical and optical spiking were computed at each frequency: * $P < 0.05$, ** $P < 0.01$ and *** $P < 0.001$.

Supplementary Figure 11

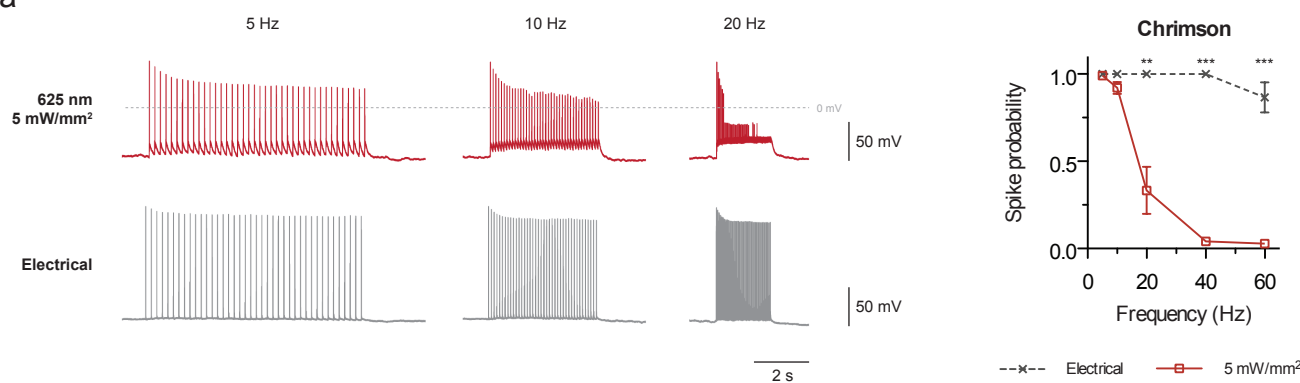


Supplementary Figure 12 – Red light driven spiking in cultured neurons.

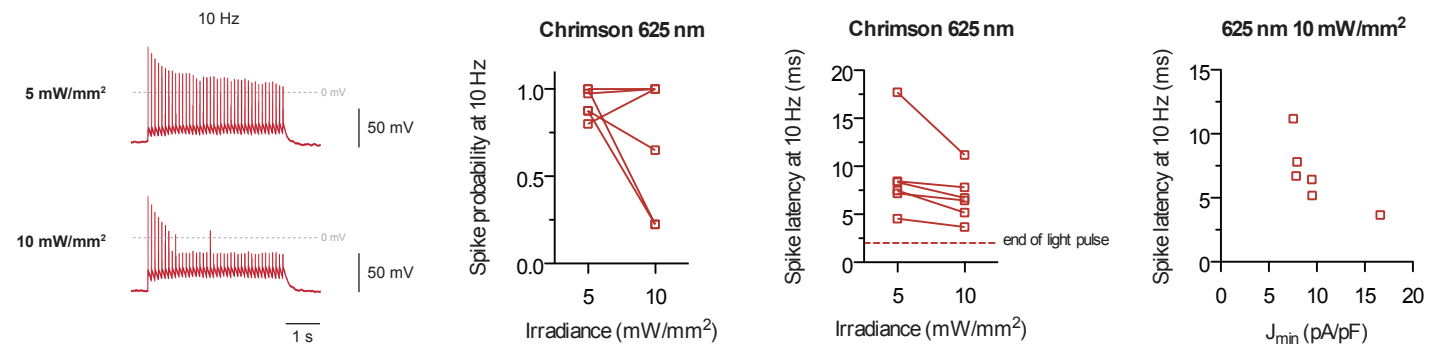
(a-d) Red (625 nm) light spike frequency data for Chrimson-expressing neurons selected based on the presence of tdTomato co-expression ($n = 6$ cells). Stimulations were as performed in Fig. 2e (train of 40 pulses, 2 ms pulse duration). **(a)** Optical vs. electrical spiking showing Chrimson can reliably drive spikes only at <20 Hz. **(b)** Chrimson's spike fidelity can decrease at higher red irradiance due to channel inactivation and/or depolarization block. **(c-d)** Spike latency, defined as light onset to spike peak, is both a function of irradiance **(c)** and Chrimson expression level **(d)**. **(e)** Action spectrum of a ChrimsonR expressing HEK293 cell ($n = 1$ cell). **(f)** Current measured at the end of 1 s light pulse (I_{\min}) for Chrimson- or ChrimsonR-expressing cultured neurons. Population mean and s.e.m. are plotted as black line. **(g)** Chronos red (625 nm) light crosstalk characterization ($n = 4$ cells). Peak voltage crosstalk for 5 ms pulses at 5 Hz and for continuous 500 ms pulse, representative cell (left) and population average (right). Statistics for **a**: Paired t-test between electrical and optical spiking were computed at each frequency: $^*P < 0.05$, $^{**}P < 0.01$ and $^{***}P < 0.001$.

Supplementary Figure 12

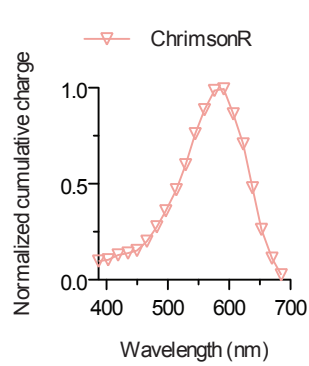
a



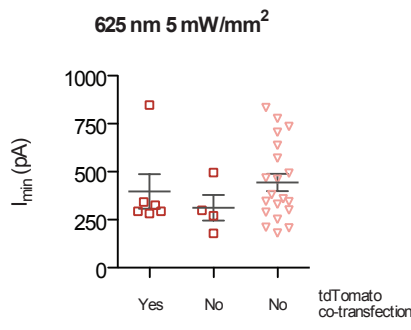
b



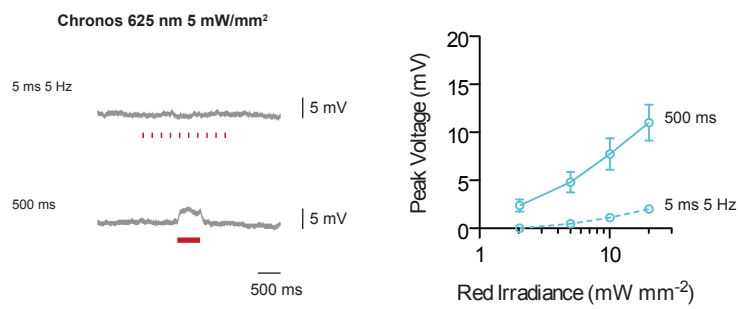
e



f



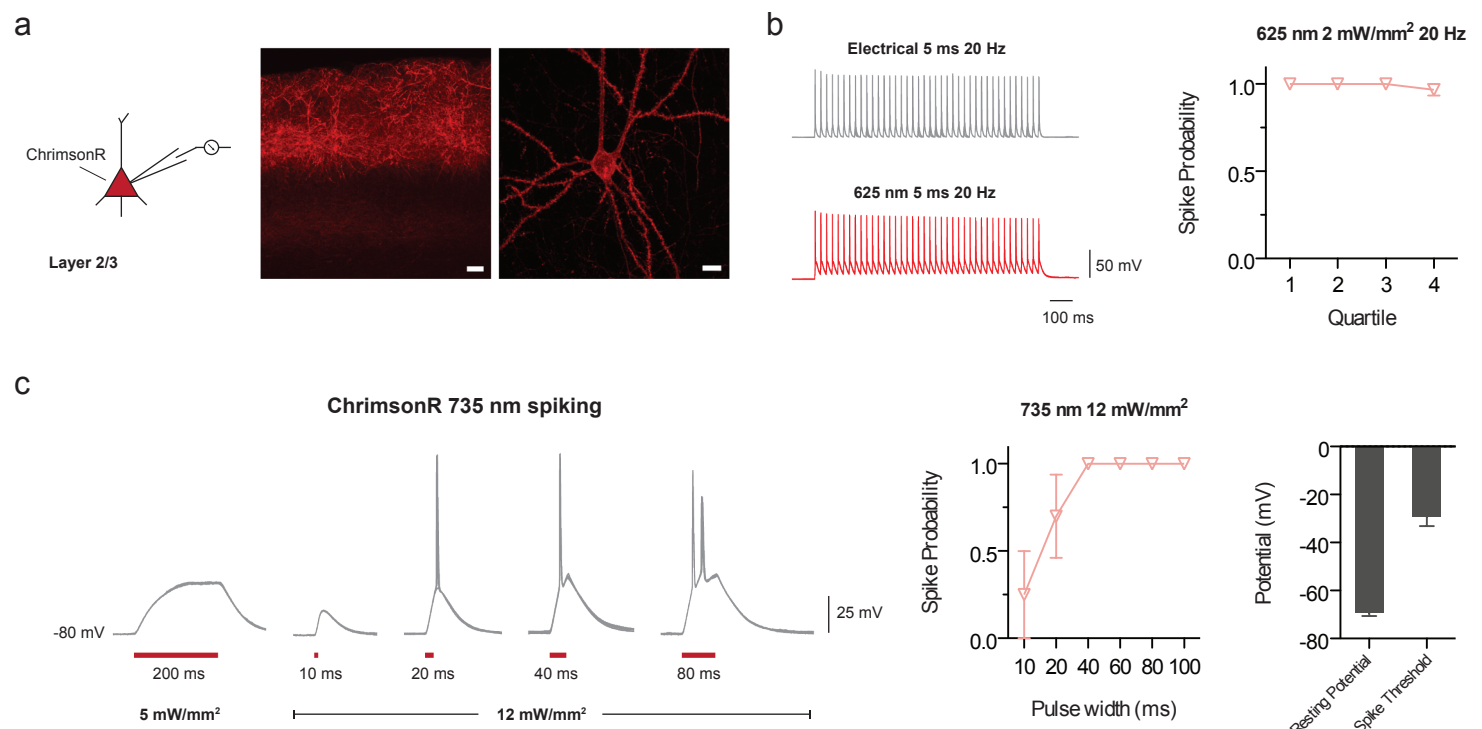
g



Supplementary Figure 13 – Red and far-red spiking with ChrimsonR in acute cortical slice.

Spectral and kinetic characterization of ChrimsonR in slice ($n = 4$ neurons from one P60 mouse throughout figure; pCAG-ChrimsonR-tdTomato was electroporated as specified in Methods). **(a)** ChrimsonR histology showing layer 2/3 expression (left, scale bar = 50 μm) and individual neuron expression (right, scale bar = 10 μm). **(b)** 625 nm spiking fidelity at 20 Hz (5 ms, 40 pulses, 3 sweeps overlaid). **(c)** Far-red 735 nm spiking with ChrimsonR (5 sweeps overlaid per condition). Traces from a representative trace from a single neuron (left), population average (middle), and membrane properties (right).

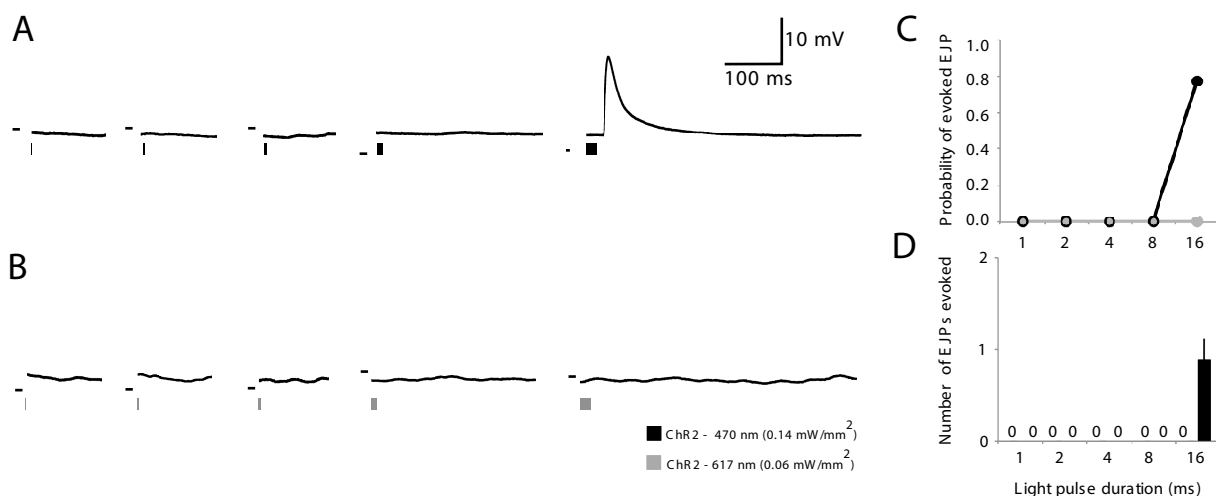
Supplementary Figure 13



Supplementary Figure 14 – Larval motor axons expressing ChR2 fire in response to blue but not red light pulses.

(a,b) Intracellular recordings from m6 muscles in 3rd instar larvae expressing ChR2 in motor neurons. Responses to 470 nm and 617 nm light pulses of increasing duration are shown. EJPs were only triggered by 16 ms pulses. Dashes in each panel indicate -50 mV. **(c)** Probability of light-evoked EJPs after 1, 2, 4, 8, and 16 ms pulses in response to 470nm and 617nm light. As in **Fig. 3d**. **(d)** Mean \pm s.e.m. number of EJPs evoked in response to light pulses. As in **Fig. 3e**. Sample size in each case: $n = 6$ muscles from 3 animals.

Supplementary Figure 14

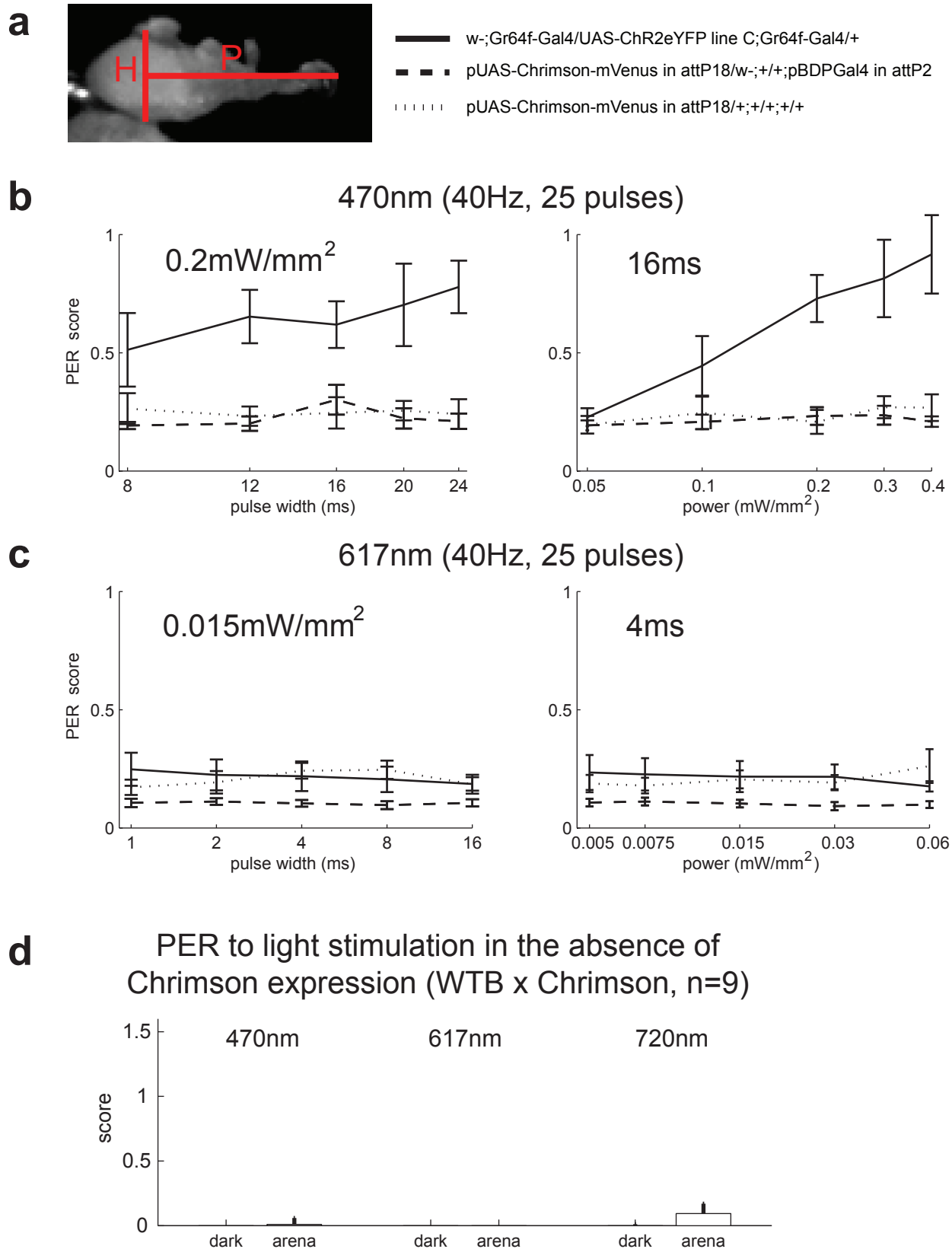


Supplementary Figure 15 – Proboscis extension reflex (PER).

(a) PER score was computed as $(P-H)/H$, where H is the pixel distance between the root of antennae and the neck connective (i.e., the head capsule) and P is the maximum horizontal pixel distance from the center of the head to the tip of proboscis during 0–2 seconds after initiation of each trial. **(b, c)** PER of three different fly groups to 25 light pulses at 470nm **(b)** and 617nm **(c)**. $n = 5$ for each population. **(d)** PER to light stimulation without Chrimson expression in sugar receptors. Data is from the same video recording analyzed for startle response in

Fig. 3g.

Supplementary Figure 15

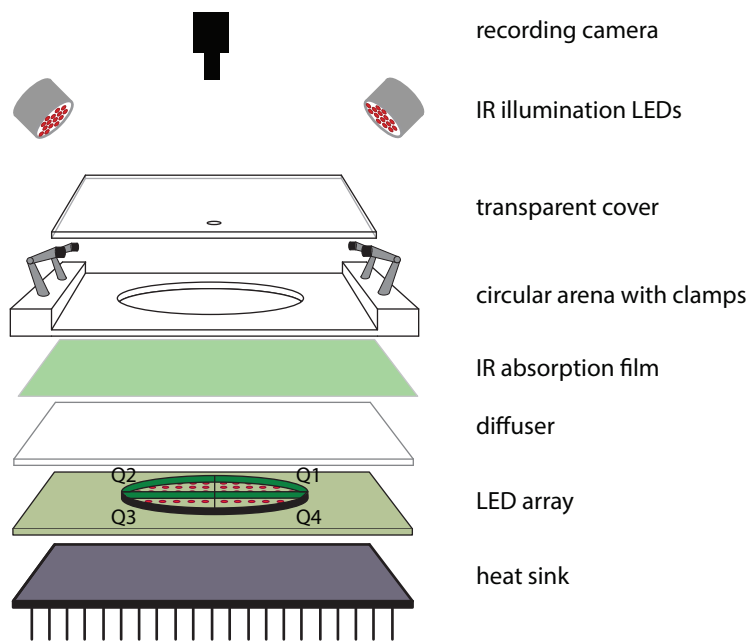


Supplementary Figure 16 – Optogenetics of freely behaving intact flies.

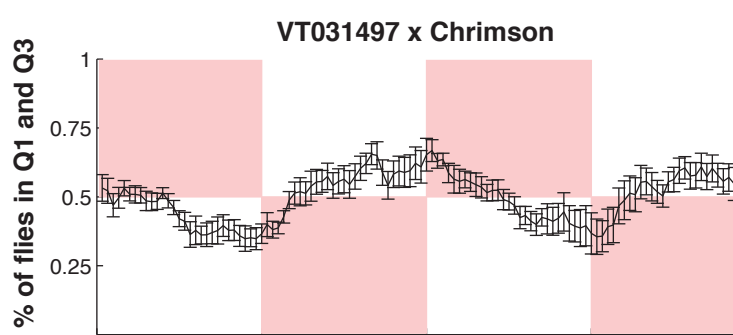
(a) Hardware configuration of a circular light arena for deep brain stimulation of freely behaving flies with intact cuticle. Note that the LED array is divided into 4 quadrants (Q1~Q4). **(b)** Fraction of flies in quadrants 1 and 3 for the experimental group. If more than 50% of flies are in the illuminated quadrants, the error bar enters into to the red-shaded zones of the plot. Flies with Chrimson expression in PNv-1 neurons avoid illuminated area. See also **Supplementary Video 6**. **(c)** Flies of control group do not avoid illuminated area.

Supplementary Figure 16

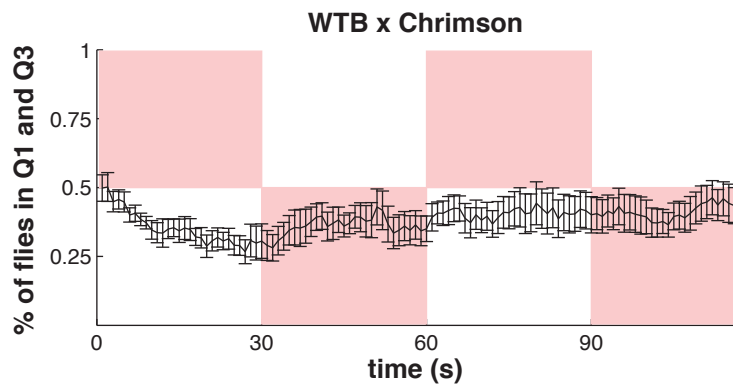
a



b



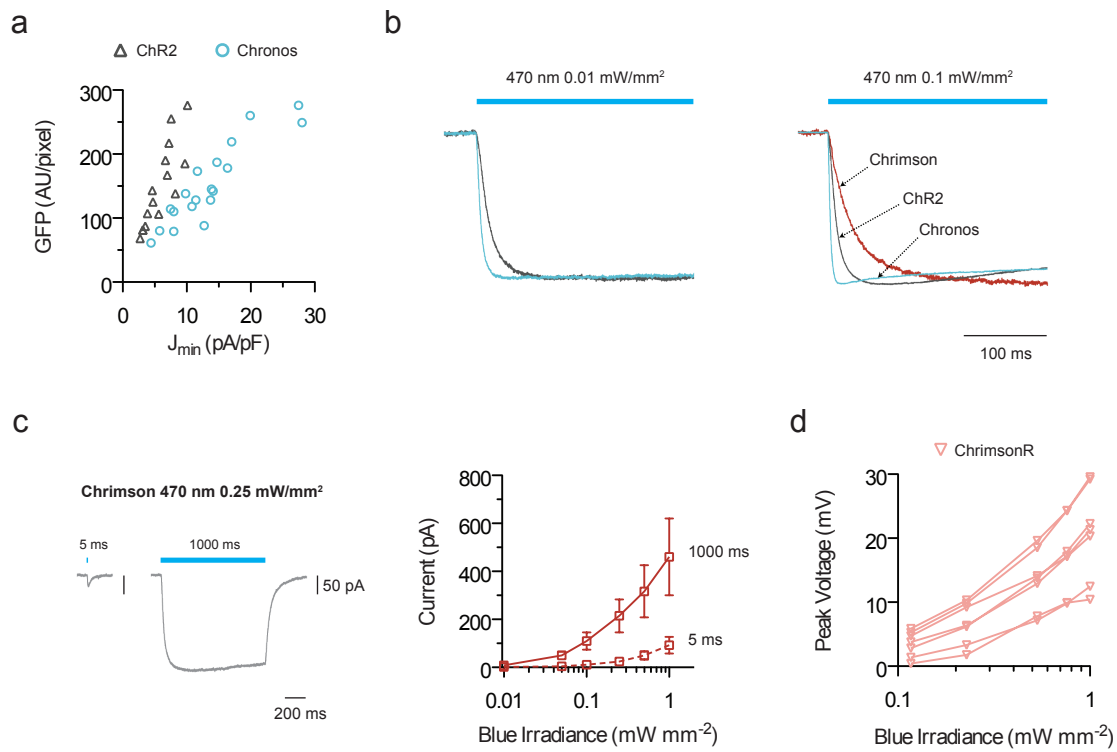
c



Supplementary Figure 17 – Two-color excitation controls in cultured neurons.

(a) Current density at end of 1 s light pulse (5 mW/mm^2 , 470 nm light) J_{\min} is defined in the same manner as **Supplementary Fig. 10c**. This is from the same dataset as **Fig. 4f**. **(b)** Averaged traces of ChR2-, Chronos-, and Chrimson-expressing neurons at the indicated irradiances of 470 nm light ($n = 4 - 7$ cells for each opsin; 1 second pulse; traces are truncated to the first half of illumination). **(c)** Chrimson blue current in response to 5 ms or 1 s pulses. Traces from a representative cell (left) and population average (right) ($n = 4$ cells). **(d)** ChrimsonR blue light voltage crosstalk for individual cells ($n = 7$ cells). Same condition as **Fig. 4b**.

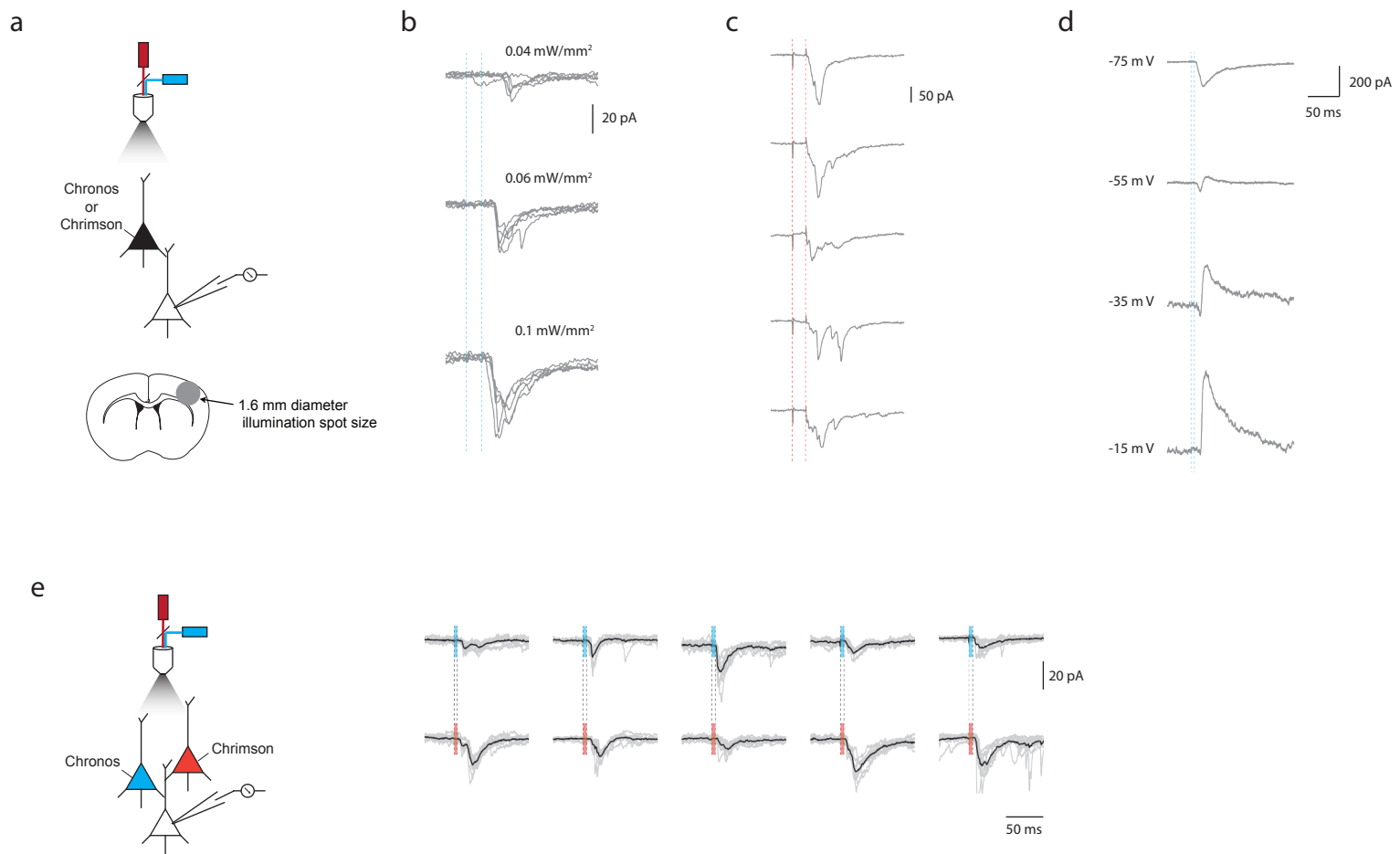
Supplementary Figure 17



Supplementary Figure 18 – Optically evoked post-synaptic currents (PSCs) in acute slice.

(a) Widefield illumination with 20x objective (1.6 mm diameter spot size at the focal plane) was used to optically drive spikes in the opsin expressing pre-synaptic neurons. Both pre- and post-synaptic neurons are in layer 2/3. **(b-d)** Either Chronos or Chrimson is expressed in the cortical brain slice; not both. All stimulations were done at 0.2 Hz. Color and irradiance are as used in **Fig. 5g-j** unless otherwise indicated. **(b)** Chronos PSC from the same neuron shows faster onset and greater amplitude (potentially with multiple PSC peaks) at higher blue irradiance. Trials are overlaid for each irradiance. Vertical dashed lines denote the start and end of 5 ms light pulse for all traces (and also providing a time scale reference). **(c)** Multiple traces, not overlaid, showing trial-to-trial variability for Chrimson PSC at 4 mW/mm² of red light. **(d)** Chronos PSC at various holding voltages shows immediate excitatory PSC followed by strong inhibitory PSC in response to 1 mW/mm² of blue light. **(e)** Red and blue light driven post-synaptic responses from five different non-expressing neurons downstream of opsin-expressing neurons, in brain slice now expressing both Chronos and Chrimson. Here, the dashed lines indicate timing, and the color of the shaded bar within, the color of light delivered. Black trace is the averaged response, grey traces are individual trials, throughout this figure.

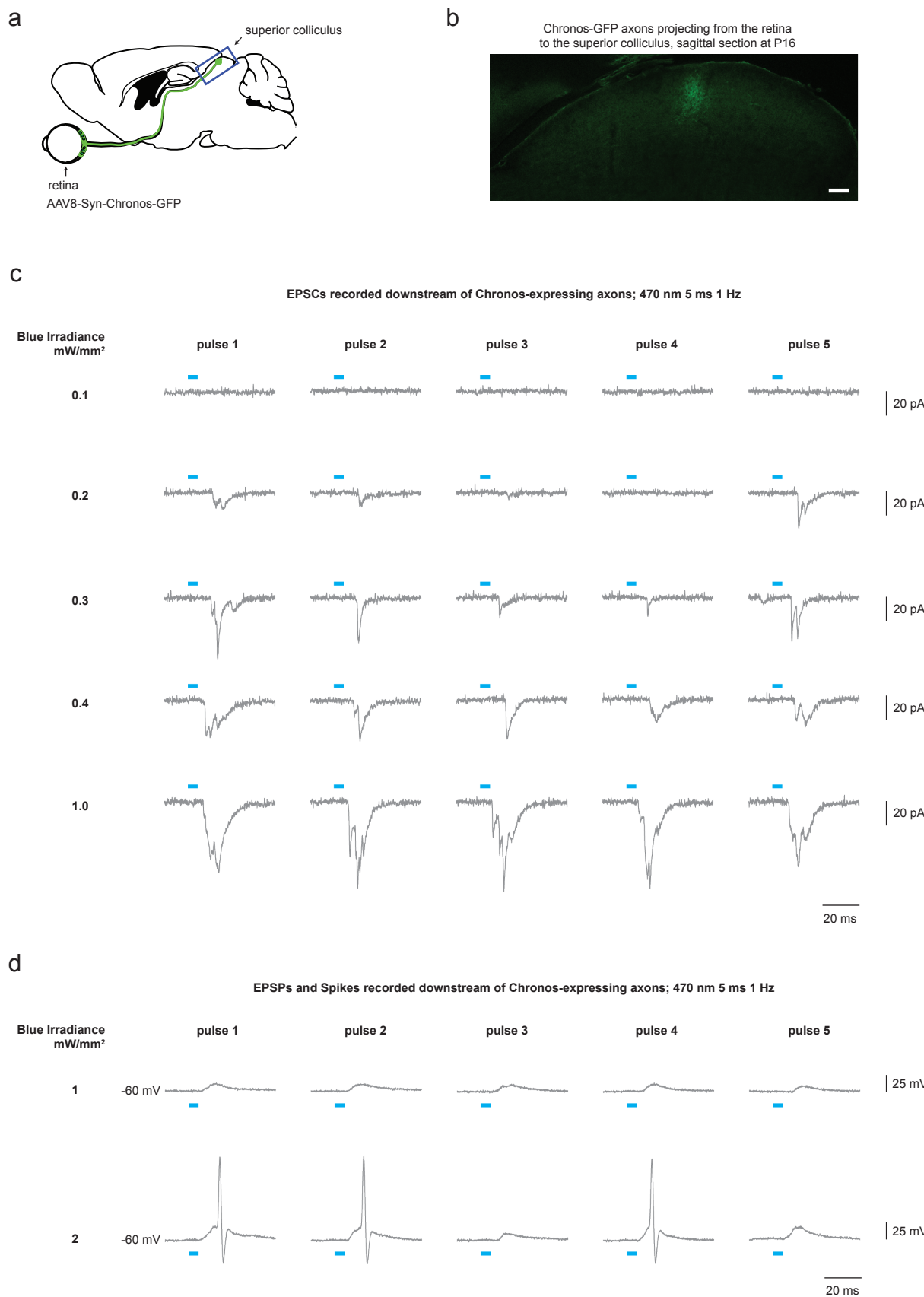
Supplementary Figure 18



**Supplementary Figure 19 – Retina to superior colliculus projection
stimulation with Chronos.**

Post-synaptic responses recorded in a superior colliculus neuron, downstream of Chronos expressed in retinal ganglion cells. See methods for retinal virus delivery details. **(a)** Diagram of retina projection to superior colliculus (adapted from ⁵¹). **(b)** Histology of Chronos-GFP axons from sagittal section of superior colliculus. Scale bar is 100 μ m. **(c-d)** Post-synaptic current and potential in response to blue light at multiple irradiances (5 pulses, 1 Hz, 5 ms pulse duration in all cases. Traces from a neuron recorded from a P18 mouse).

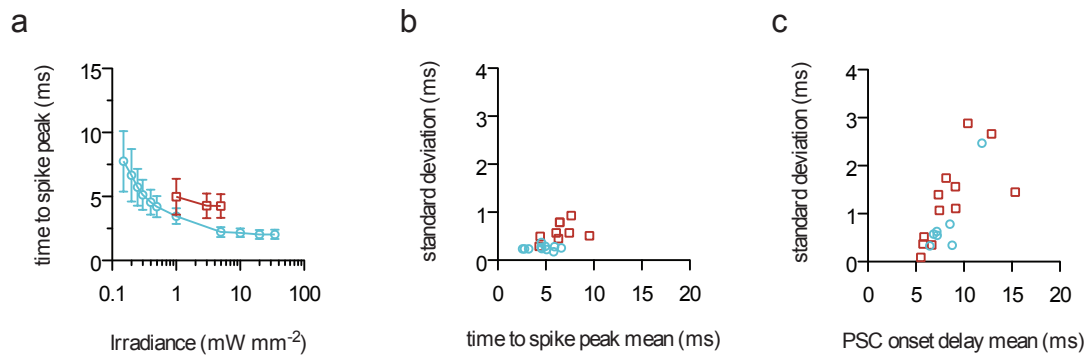
Supplementary Figure 19



Supplementary Figure 20 – Comparisons of spiking and post-synaptic response timing in acute slice.

(a) Time-to-spike-peak as a function of irradiance when optically driving Chrimson neurons in the red and Chronos neurons in the blue; color and pulse duration as in **Fig. 5b-d**. Values shown are population average \pm standard deviation. In all subpanels, red squares denote Chrimson, blue circles denote Chronos ($n = 9$ cells, 3 mice, Chrimson; $n = 11$ cells, 4 mice, Chronos). **(b)** Time-to-spike-peak for individual Chronos- (0.3 mW/mm² blue light) and Chrimson-expressing (5 mW/mm² red light) neurons. Values are trial mean and standard deviation (cells patched from 3-4 mice for each opsin). **(c)** Post-synaptic current latency (time from beginning of light pulse, to 10% of synaptic current peak) for individual neurons post-synaptic to Chronos (0.3 mW/mm² blue) or post-synaptic to Chrimson (4 mW/mm² red). Values shown are trial averages and standard deviation (cells patched from 2-4 mice for each opsin).

Supplementary Figure 20



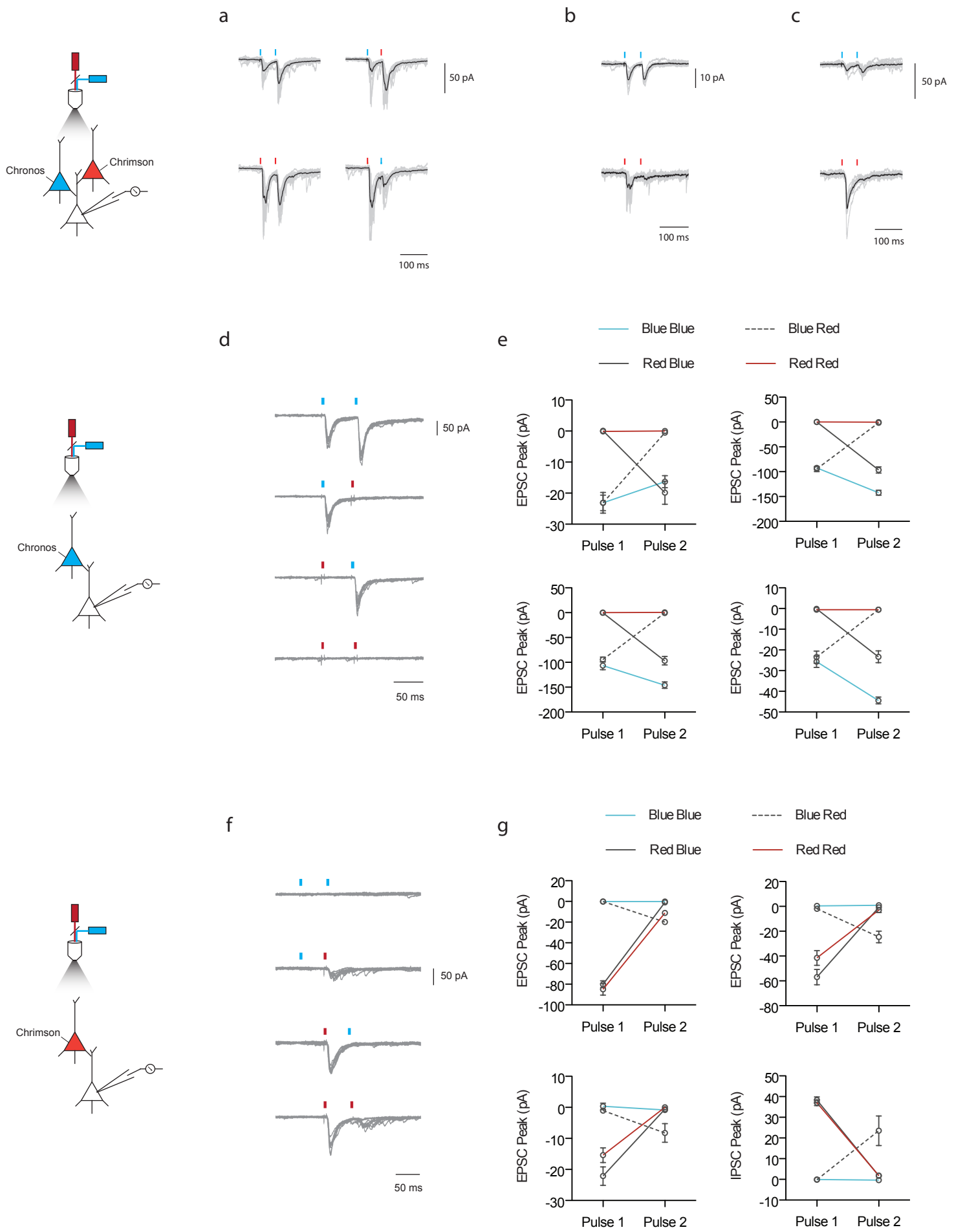
Supplementary Figure 21 – Optically evoked paired-pulse responses in acute slice.

(a-c) Chrimson and Chronos expressed in separate neurons in the same slice using triple plasmid *in utero* electroporation. Patched neurons are post-synaptic to both Chrimson and Chronos based on optical response to blue and red light.

(a) Paired-pulse responses (PPR) for an exemplar neuron. Blue-blue stimulation exhibited facilitation, while other paired pulses were linear summation of individual pulse response. 470 nm, 0.2 mW/mm²; 625 nm, 1 mW/mm². 5 ms pulse width and inter-pulse interval 50 ms throughout this figure. Black trace is the averaged response, grey traces are individual trials, throughout this figure.

(b-c) Blue-blue and red-red responses from the same neuron showed no differences in the blue paired PSC, while the second red pulse response often failed at 50 ms. 470 nm, 0.37 mW/mm²; 625 nm, 1mW/mm². **(d-g)** Chrimson and Chronos expressed in separate slices. 470nm, 0.3 mW/mm², 625 nm, 4 mW/mm² used throughout. **(d-e)** PPR recorded downstream of Chronos-expressing neurons. Representative trace **(d)** and averaged PPR in four different neurons **(e)**, showing reliable Chronos drive . **(f-g)** PPR recorded downstream of Chrimson-expressing neurons. Representative trace **(f)** and averaged PPR in four different neurons **(g)**, showing second pulse fails due to kinetic limitation of Chrimson. An inhibitory PSC (voltage clamped at -55 mV) was recorded from one neuron, most likely due to mistargeting during *in utero* electroporation.

Supplementary Figure 21

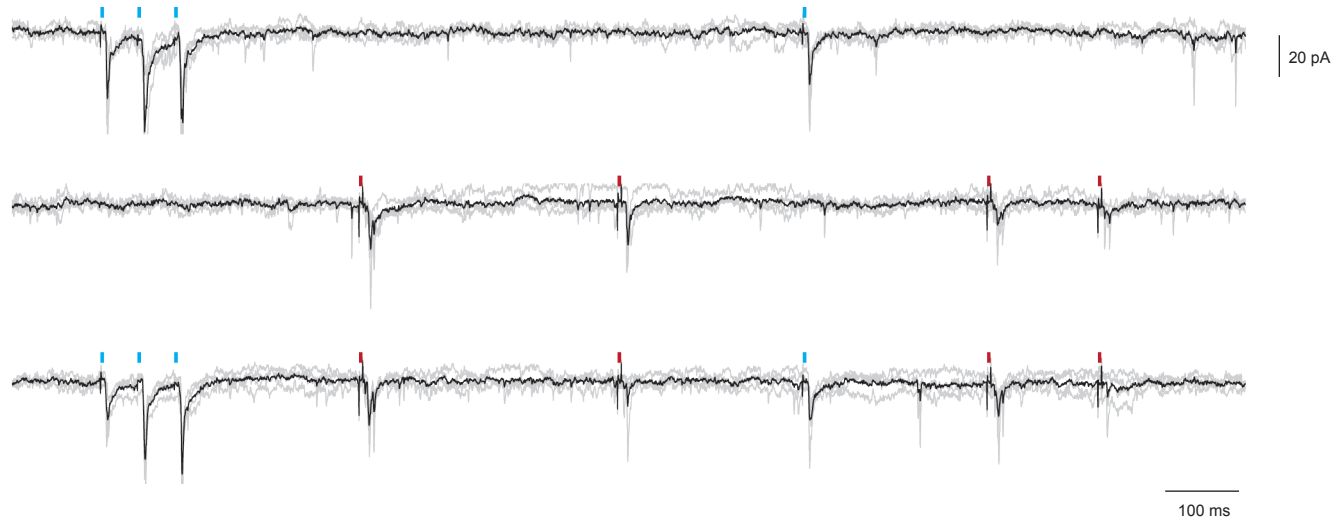


Supplementary Figure 22 – Post-synaptic current raw traces.

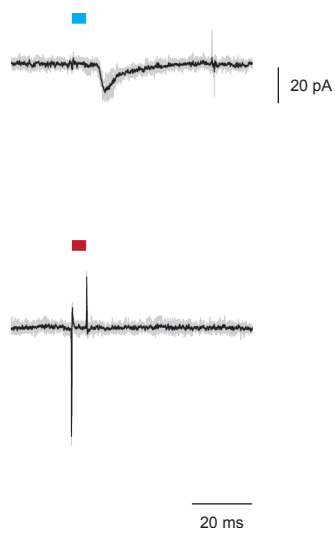
Unfiltered traces with LED stimulation artifact. Panel **(a)**, **(b)**, and **(c)** corresponds to the filtered traces in **Fig. 5g, h, and i** respectively.

Supplementary Figure 22

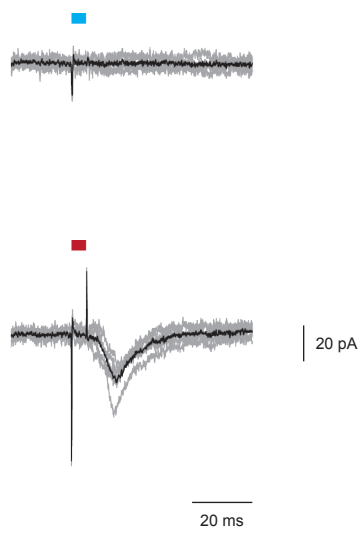
a



b



c



Supplementary Table 1 – Naming convention

Gene #	NCBI #	Alias	Genus	species
		ChR1	Chlamydomonas	reinhardtii
		ChR2	Chlamydomonas	reinhardtii
		VChR1	Volvox	carteri
		MvChR1	Mesostigma	viride
60	KF992067		Mesostigma	viride
62	KF992054	NsChR	Neochlorosarcina	sp.
63	KF992043		Monomastix	opisthostigma
64	KF992072	SdChR	Scherffelia	dubia
65	KF992034	BsChR2	Brachiomonas	submarina
66	KF992089	TsChR	Tetraselmis	striata
67	KF992071		Tetraselmis	chui
68	KF992081		Tetraselmis	chui
69	KF992087		Tetraselmis	chui
70	KF992084		Spermatozopsis	exsultans
71	KF992066		Pedinomonas	minor
72	KF992045		Cyanophora	paradoxa
73	KF992053		Stephanosphaera	pluvialis
74	KF992059	HdChR	Haematococcus	droebakensis
75	KF992058		Tetraselmis	striata
76	KF992070		Tetraselmis	chui
77	KF992057	TcChR	Tetraselmis	cordiformis
78	KF992042		Pavlova	lutheri
79	KF992077		Scherffelia	dubia
80	KF992086	BsChR1	Brachiomonas	submarina
84	KF992047		Rhodomonas	sp.
85	KF992030		Chloromonas	reticulata-A
86	KF992041	CoChR	Chloromonas	oogama
87	KF992078	CsChR	Chloromonas	subdivisa
88	KF992060	CnChR1/Chrimson	Chlamydomonas	noctigama
89	KF992073	CnChR2	Chlamydomonas	noctigama
90	KF992040	ShChR/Chronos	Stigeoclonium	helveticum
91	KF992032		Microthamnion	kuetzianum-A
92	KF992049		Chlamydomonas	bilatus-A
93	KF992052		Heterochlamydomonas	inaequalis
95	KF992076		Chloromonas	reticulata-A
96	KF992036		Chlamydomonas	noctigama
97	KF992074	PsChR1	Proteomonas	sulcata
98	KF992083		Cryptomonas	curvata

99	KF992085		Chroomonas	sp.
100	KF992088		Chroomonas	sp.
101	KF992051		Chroomonas	sp.
102	KF992090		Chroomonas	sp.
103	KF992033		Proteomonas	sulcata
104	KF992065		Chroomonas	sp.
105	KF992064		Gloeochaete	wittrockiana
106	KF992061		Hemiselmis	virescens
107	KF992055		Proteomonas	sulcata
108	KF992056	PsChR2	Proteomonas	sulcata
109	KF992063		Proteomonas	sulcata
110	KF992037		Rhodomonas	sp.
111	KF992044		Chlamydomonas	bilatus-A
112	KF992038	AgChR	Asteromonas	gracilis-B
113	KF992046		Pyramimonas	parkeae
114	KF992035		Monomastix	opisthostigma
115	KF992079		Tetraselmis	striata
116	KF992075		Lobomonas	rostrata
117	KF992031		Lobomonas	rostrata
118	KF992050		Stichococcus	bacillaris
119	KF992080		Hafniomonas	reticulata
120	KF992062	CbChR1	Chlamydomonas	bilatus-A
121	KF992039		Hafniomonas	reticulata
122	KF992069		Carteria	crucifera
123	KF992048		Carteria	crucifera
124	KF992068		Volvox	aureus
125	KF992082		Phacotus	lenticularis

Supplementary Table 2 – Primer sequences

Primers for generating cDNA library

Name	Sequence	Comment
RNA adapter 2	AAUCAUACGACGACCACCGAGAUCAGG	5' mRNA ligation adaptor
DNA adapter 1	AAGCAGTGGTATCAACGCAGACTAC(T) ₃₀ VN	Reverse transcription

Primers for algae PCR

Name	Sequence
DNA adapter 2	AATCATACGACGACCACCGAGATCAGG
55 GSP5	GAAACACCTCAATCATCACCTTGACC
55 GSP6	CAGCCTGTCCCGCATCACAGGAACG
55 GSP8	CGGGCTTACAAGACCAGTACAGCAAG
2565 GSP12	ATCTTGACCTGGAGGTAATGGGCG
232 GSP6	GTGATAATCTGATTAAGCCGTGGCG
51 GSP2	CGTTCAGCCCCGTTATATTCGATAG
1293 GSP2	AAAAGCAGCCGATGTAGAAGAGGAGC
CCAC19 GSP1	TACGCTACCTCCTTGTGGTGGAG
CCAC19 GSP2	GTAGTCCACACCACTATCGTCAGCAG

Primer pairs for algae PCR

Gene #	Algae source	Template	Primer 1	Primer 2
74	UTEX 55	cDNA	DNA adapter 2	55 GSP5
		cDNA	55 GSP8	55 GSP6
75	UTEX 2565	cDNA	DNA adapter 2	2565 GSP12
76	UTEX 232	cDNA	DNA adapter 2	232 GSP6
77	CCAC 51	cDNA	DNA adapter 2	51 GSP2
78	UTEX 1293	cDNA	DNA adapter 2	1293 GSP2
79	CCAC 19	genomic DNA	CCAC19 GSP1	CCAC19 GSP2

UTEX: <http://web.biosci.utexas.edu/utex/>

CCAC: <http://www.ccac.uni-koeln.de>

Primers for cloning

Name	Sequence
Cloning P12	GGAGGTGGAAGTGGAAAGAGTCGTGGAGG
Cloning P13	actaggtacccaggtaCTTATACAGCTCATGCCATGCCGTACAG
Cre P1	caaaGAATTCTgagcccccaccATGcccaagaagaagaggaagggttccAATTACTGACCGTAC ACCAAAATTGCGC
Cre P2	ggacccgcaccactccgcccaccagaATGCCATCTCCAGCAGGC
Cre P3	GGCTTCTGGCGTGTGACC
GB1 (dsDNA)	CTGTCTCATCATTGGCAAAGAACATTCCCATAACCTCGTATAAAGTATCCTATACG AAGTTATATCAAAATAGGAAGACCAATGCTTCACCATCGACCCGAATTGCCAAGC ATCACCATCGACCCATAACTCGTATAATGTATGCTATACGAAGTTACTAGCTA GCGCCGCCACCATGGAAACAGC
GB2 (dsDNA)	GAGCTGTACAAGTAATGAGCGGCCTAGGTACCTAGTATAACCTCGTATAAGGATA CTTTATACGAAGTTATCATTGGGATTCTTCTATTGATCCAAGCATCACCATCG ACCCCTAGTCCAGATCTCACCATCGACCCATAACTCGTATAAGCATACATTATA CGAAGTTATGTCCTCGAAGAGGTTCGCGGCCACTCCTCAGGTGCAG
Gene88 P2	ctactaccggcgccgcCACTGTGTCCTCGTCCTCCTCC
Gene88 P27	actagctagccgcaccATGGCTGAGCTGATCAGCAGCG
Gene90 P9	gccgccaccATGGAAACAGCCGCCACAATGAC
Gene90 P10	actaggtacccaggccgcgcaccATGGAAACAGCCGCCACAATG
GFP P18	ggccgcatttaCTTGTACAGCTCGTCCATGCCGAG
GFP P20	actagctagTCATTACTTGTACAGCTCGTCCATGC
OE P1	CTGTCTCATCATTGGCAAAGAACATTCCC
OE P2	CTGCACCTGAGGAGTGCAGGCCCG
OE P13	CAGTGccggcaccggtagtagcaGTGAGCAAGGGCGAGGAGA
OE P14	actaggtacccaggccgtatttaCTTGTACAGCTCGTCCATGCCG
OE P15	ACTAGCTAGCGCCGCCACCATGG
OE P16	ACTAGGTACCTAGGCCGCTCATTAC
tdTomato P1	ctgcacccggtagtagcaGTGAGTAAGGGCGAGGAAGTGATCAAAG
tdTomato P2	gagtgcggccgtttaCTTATACAGCTCATGCCATGCCGTACAGAAC

Supplementary Video 1 – Experimental setup with a visual arena.

The fly was tethered and centered in the visual arena⁵⁰. In this movie, a flowing random dot pattern is shown. The visual arena was removed from the setup in other conditions. Fly behavior was recorded using a camera with 850 nm IR illuminator.

Supplementary Video 2 – PER of a Gr64f X Chrimson fly to 720 nm light in darkness.

A fly with Chrimson expression in sugar receptors shows PER to deep red light stimulation.

Supplementary Video 3 – Startle response to 720 nm light in darkness

A control fly without Chrimson expression shows clear startle response to deep red light.

Supplementary Video 4 – PER of a Gr64f X Chrimson fly to 720 nm light in a blue random dot arena.

PER of a fly with Chrimson expression in sugar receptors is not affected by visual distractors.

Supplementary Video 5 – Inhibited startle response to 720 nm light in a blue random dot arena.

The startle response of a control fly without Chrimson expression is effectively inhibited.

Supplementary Video 6 – Optogenetics in freely behaving intact flies.

Top: Light-induced CO₂ avoidance behavior (VT031497-Gal4 x UAS-Chrimson in attP18). Bottom: A control group (WTB x UAS-Chrimson in attP18). Circles show raw video images with false color red background indicating the illuminated quadrants. The effect of light is quantified (see Methods) and plotted as a single blue line corresponding to the presented examples and a plot representing the mean of all 9 sessions (\pm SEM error bars). Plots will be in red region if more than 50% of flies are in illuminated quadrants. Replay speed: 4x.